UNIVERSITY OF LEEDS

This is a repository copy of *Anatomy and dimensions of fluvial crevasse-splay deposits: examples from the Cretaceous Castlegate Sandstone and Neslen Formation, Utah, U.S.A.*.

White Rose Research Online URL for this paper:
http://eprints.whiterose.ac.uk/112018/

Version: Accepted Version

Article:

Burns, CE, Mountney, NP orcid.org/0000-0002-8356-9889, Hodgson, DM orcid.org/0000-0003-3711-635X et al. (1 more author) (2017) Anatomy and dimensions of fluvial crevasse-splay deposits: examples from the Cretaceous Castlegate Sandstone and Neslen Formation, Utah, U.S.A. Sedimentary Geology, 351. pp. 21-35. ISSN 0037-0738

https://doi.org/10.1016/j.sedgeo.2017.02.003

© 2017 Published by Elsevier B.V. This manuscript version is made available under the CC-BY-NC-ND 4.0 license http://creativecommons.org/licenses/by-nc-nd/4.0/

Reuse
Unless indicated otherwise, fulltext items are protected by copyright with all rights reserved. The copyright exception in section 29 of the Copyright, Designs and Patents Act 1988 allows the making of a single copy solely for the purpose of non-commercial research or private study within the limits of fair dealing. The publisher or other rights-holder may allow further reproduction and re-use of this version - refer to the White Rose Research Online record for this item. Where records identify the publisher as the copyright holder, users can verify any specific terms of use on the publisher's website.

Takedown
If you consider content in White Rose Research Online to be in breach of UK law, please notify us by emailing eprints@whiterose.ac.uk including the URL of the record and the reason for the withdrawal request.

White Rose
university consortium
Universities of Leeds, Sheffield & York

eprints@whiterose.ac.uk
https://eprints.whiterose.ac.uk/

Anatomy and dimensions of fluvial crevasse-splay deposits: examples from the Cretaceous Castlegate Sandstone and Neslen Formation, Utah, U.S.A.

Burns, C., Mountney, N.P., Hodgson, D.M., and Colombera, L.

Fluvial and Eolian Research Group, School of Earth and Environment, University of Leeds, Leeds, LS170AN, UK

Email:ee09ceb@leeds.ac.uk

Abstract

Crevasse-splay deposits form a volumetrically significant component of many fluvial overbank successions (up to 90% in some successions).Yet the relationships between the morphological form of accumulated splay bodies and their internal facies composition remains poorly documented from ancient successions. This work quantifies lithofacies distributions and dimensions of exhumed crevasse-splay architectural elements in the Campanian Castlegate Sandstone and Neslen Formation, Mesaverde Group, Utah, USA, to develop a depositional model. Fluvial crevasse-splay bodies thin from 2.1 m (average) to 0.8 m (average) and fine from a coarsest recorded grain size of lower-fine sand to fine silt away from major trunk channel bodies. Internally, the preserved deposits of splays comprise laterally and vertically variable sandstone and siltstone facies associations:

proximal parts are dominated by sharp and erosional-based sandstone-prone units, which may be Structureless or may comprise primary current lineation on beds and erosional gutter casts; medial parts comprise sets of climbing-ripple strata and small scale deformed beds; distal parts comprise sets of lower-stage plane beds and complex styles of lateral grading into fine-grained floodbasin siltstones and coals. Lithofacies arrangements are used to establish the following: (i) recognition criteria for crevasse-splay elements; (ii) criteria for the differentiation between distal parts of crevasse-splay bodies and flood plain fines; and (iii) empirical relationships with which to establish the extent (ca. 500 m long by 1000 m wide) and overall semi-elliptical planform shape of crevasse-splay bodies. These relationships have been established by high-resolution stratigraphic correlation and palaeocurrent analysis to identify outcrop orientation with respect to splay orientation. This permits lateral changes in crevasse-splay facies architecture to be resolved. Facies models describing the sedimentology and architecture of crevasse-splay deposits preserved in floodplain successions serve as tools for determining both distance from and direction to major trunk channel sandbodies.

Keywords: Mesaverde Group, overbank, crevasse-splay, fluvial, facies analysis.

1. Introduction

Crevasse-splay deposits form a volumetrically significant part of fluvial overbank depositional elements, representing on average ~12% of all deposits in ancient preserved fluvial successions (Colombera et al., 2013). Despite this, the preserved lithofacies arrangement and stratigraphic architecture of fluvial overbank successions generally, and crevasse-splay elements in particular, have been less of a focus of analysis than in-channel deposits (e.g. Bridge, 1984, 2006, Colombera et al., 2012). Many published fluvial facies models generalize crevasse-splay deposits into a single category (e.g. Miall, 1985, 1988, 2014, Bridge, 2006, Ghazi and Mountney, 2009, 2011, Colombera et al., 2013); relatively few studies have specifically set out to undertake a detailed lithofacies characterization and architectural-element analysis of splay deposits. O'Brien and Wells (1986), Bristow et al. (1999), Farrell (2001) and Li and Bristow (2015) examined the sedimentology of modern and recent crevasse-splay deposits, and Mjøs et al. (1993), Behrensmeyer et al. (1995), Jones and Hajek (2007), Widera (2016) and Van Toorenenburg (2016) presented examples of ancient crevasse-splay deposits. Detailed lithofacies classification schemes have been introduced for modern avulsion deposits, for example in the Cumberland Marshes, Canada (Perez-Arlucea, 1999), and for Miocene coal-prone crevasse-splay successions in Poland (Widera, 2016).

This study presents a depositional model to account for the complexity of lithofacies distribution preserved in crevasse-splay deposits that accumulated under the influence of a greenhouse climatic regime. This aim is fulfilled through an outcrop-based quantitative geometrical analysis of 35 crevasse-splay bodies present in the Cretaceous (Campanian) Castlegate Sandstone and Neslen Formation of the Mesaverde Group, eastern Utah, USA. This study seeks: (i) to establish recognition criteria of architectural elements that represent fluvial crevasse splay deposits, and to contrast these elements with overbank elements dominated by suspension settling in floodbasin settings; (ii) to demonstrate how and why these facies are arranged within an individual preserved crevasse-splay element; (iii) to quantify proportions and dimensions of crevasse-splay elements versus floodplain elements in a greenhouse overbank succession; and (iv) to develop a predictive facies model for crevasse-splay element architecture based on observations from examples identified in the Castlegate Sandstone and Neslen Formation.

2. Background and nomenclature

The fluvial floodplain is a geomorphic feature defined as a low-gradient area of alluvium adjacent to a channel belt and that is affected by fluvial flooding; sediment is dominantly supplied via floods that cause rivers to breach the confines of trunk channel systems (Brierley and Hickin, 1992, Nanson and Croke, 1992, Bridge, 2006, Bridge and Demicco, 2008). In the stratigraphic record, the fluvial overbank is a gross-scale composite architectural element that comprises any part of a fluvial system that accumulates sediment outside the confines of the river channel (Miall, 1996, 2014). The fluvial overbank is characterized by a range of smaller-scale sub-environments, including crevasse channels, crevasse splays, floodbasins, mires and lakes or ponds; these sub-environments, and their preserved expression as architectural elements in the rock record, comprise a range of sediment types of physical, chemical and biogenic origin (e.g., Brierley and Hickin, 1992; Platt and Keller, 1992; Brierley, 1997; Hornung and Aigner, 1999). Typically, the fluvial overbank comprises sediments that are finer than those associated with intra-channel deposits (Miall, 1993). Many overbank sub-environments and their preserved deposits are subject to pedogenesis, which is strongly controlled by the drainage state of the substrate at the time of accumulation (Bown and Kraus, 1987; Kraus, 1999) and the sedimentary stability of the land surface.

In fluvial sedimentary environments, a splay deposit is defined as a sheet-like progradational deposit, which is lobe-shaped in plan-view. Terminal splay deposits form at the end of a river channel whereas crevasse splay deposits, which are the focus here, form adjacent to an established channel (e.g. Nichols and Fisher, 2007; Gulliford et al. 2014). Typically, crevasse splays initiate and develop when floodwaters break through a topographically elevated levee that acts as the confining bank of a channel at times of peak flood discharge or when floodwaters overtop the levee (Coleman, 1969; Mjøs et al., 1993; Arnaud-Fassetta, 2013) (Fig. 1). Sediment-laden flows expand and decelerate as they pass through a distributive network of crevasse channels onto the unconfined floodplain, thereby encouraging sediment deposition (Arndorfer, 1973; Miall, 1985, 1993; Bristow et al., 1999;; Arnaud-Fassetta, 2013). Although also documented from freshwater deltaic (e.g., Arndorfer, 1973; Cahoon et al., 2011), interdistributary bay-fill (e.g., Gugliotta et al., 2015), estuarine (e.g., Staub and Cohen, 1979; Cloyd et al., 1990; Baeteman et. al, 1999), and deep-marine (Morris et al., 2014) environments, crevasse splays are most widely documented from the low-relief, low-gradient parts of fluvial systems (Mjøs et al., 1993; Bristow et al., 1999; Anderson, 2005). The majority of previous research on crevasse splay deposits has focused on modern fluvial systems (Coleman 1969; Smith et al., 1989; Farrell 2001; Smith and Perez-Arlucea, 2004; Arnaud-Fassetta, 2013). Splay evolution in modern systems has been categorized using a three-stage model based on observations by Smith et al. (1989) from the Cumberland Marshes, Canada, where simple lobate splays (type I) are typically succeeded by splays with a more fully developed network of distributary channels in which sediment is directed to localised areas within the developing splay (type II). Over time, growth and evolution of the splays tends to lead to the development of an anastomosing channel pattern (type III). There are two possible fates of mature splays: (i) detachment (cut-off) from the main parent fluvial channel, resulting in abandonment and stabilization by surface agents such as vegetation or chemically precipitated crusts or bio-chemical soils (Arnaud-Fassetta, 2013); or (ii) further development such that an active splay serves as the initial phase of a major avulsion of the parent channel (Smith et al., 1989; Jones and Harper, 1998; Farrell, 2001; Buehler at al., 2011). In cases where splays mark the initiation phase of a channel avulsion, they are referred to as avulsion splays (Smith et al., 1989; Slingerland and Smith, 2004; Jones and Hajek, 2007). In these instances, local erosion of the parent channel bank forms a crevasse channel through which sediment and water are diverted. As the discharge of water and sediment through a crevasse channel increases, the parent river may eventually avulse to take a new course through this new channel path (Bristow et al., 1999; Mohrig et al., 2000; Miall, 2014). In-channel accretion and levee construction leads to superelevation of the channel and channel perching above the floodplain, an unstable situation that promotes the triggering of avulsion (Mohrig et al., 2000). In the rock record, such evolution is manifest as a transitional avulsion stratigraphy (Jones and Hajek, 2007): crevasse-splay deposits underlie a new main channel and both the splay and the succeeding channel bodies exhibit similar overall palaeocurrent trends (Bristow et al., 1999; Mohrig et al., 2000; Slingerland, 2004; Jones and Hajek, 2007; Miall, 2014).

3. Geological setting

The Cretaceous (Campanian to Maastrichtian) Mesaverde Group, eastern Utah, USA, accumulated under the influence of a humid, subtropical, greenhouse climate. Sediment transport was eastward from the developing Sevier Orogen to the shoreline of the Western Interior Seaway that developed in the foreland of the orogeny

(Franczyk et al., 1990; Miall, 1993). This resulted in the accumulation of an eastward-prograding clastic wedge that was constructed along the western margin of the Western Interior Seaway during the Campanian (Miall, 1993; Olsen et al., 1995; Van Wagoner, 1995; Kirschbaum and Hettinger, 2004; Adams and Bhattacharya, 2005; Hampson et al., 2005; Aschoff and Steel, 2011). The Mesaverde Group comprises informal lower and upper sections, separated by the Buck Tongue of the Mancos Shale (Franczyk, 1990; Kirschbaum and Hettinger, 2004) (Fig. 2). Outcrops of the Upper Mesaverde Group, and specifically the Castlegate Sandstone and Neslen Formation, are the focus of this study.

The Castlegate Sandstone is up to 160 m thick and comprises tens of metres thick amalgamated sheets of sandstones of predominantly fluvial channel origin, with few laterally extensive bodies of overbank fines (McLaurin and Steel, 2007). In contrast, the Neslen Formation, which is up to 200 m thick, comprises a succession of conglomerate, sandstone, siltstone and coal of non-marine, paralic and shallow-marine origin (Franczyk, 1990; Hettinger and Kirschbaum, 2003).

The Castlegate Sandstone and Neslen Formation merge westward near the town of Green River into a single unit of fluvial origin: the Upper Castlegate Sandstone (Franczyk et al., 1990; Willis, 2000) (Fig. 2). Eastward, the Castlegate Sandstone is finer grained and passes downdip into the offshore marine Mancos Shale. In Colorado, deposits equivalent to the Neslen Formation take the name of the Ilês Formation (Kirschbaum and Hettinger, 2004). The Castlegate and

Neslen formations are well exposed in a series of outcrops in the Book Cliffs, Eastern Utah (Fig. 3A), between Green River and Thomson Springs (Fig. 3B). Numerous canyons yield exposures in a variety of orientations that allow for the three-dimensional geometry and internal facies arrangement of architectural elements to be constrained via lateral tracing over many hundreds of metres to kilometres.

The Castlegate Sandstone is commonly interpreted as the accumulated deposits of low- to moderate-sinuosity braided rivers (McLaurin and Steel, 2007). In contrast, the Neslen Formation represents the accumulated deposits of a series of lower-alluvial-plain, coastal-plain and near-coast fresh-to-brackish water environments that were traversed by relatively small, shallow, sinuous rivers that migrated and avulsed across extensive, low-gradient and low-relief floodplains (Franczyk, 1990; Willis, 2000; Kirschbaum and Hettinger, 2004; Cole, 2008; Aschoff and Steel, 2011b; Shiers et al., 2014; Keeton et al., 2015; Colombera et al., 2016).

Previous research has focused on the development of a robust stratigraphic framework (e.g., Franczyk, 1990; Hettinger and Kirschbaum, 2002), which is useful to place the crevasse-splay architectural elements studied here within a broader palaeoenvironmental and sequence stratigraphic context. Much previous research has been focused on the arrangement and stacking pattern of larger-scale channel and point-bar elements within the Neslen Formation (Kirschbaum and Hettinger 2002; Shiers et al., 2014; Keeton et al., 2015). However, the sedimentology and architecture of elements of crevasse-splay origin have not been considered in detail.

4. Data and methods

Here, we present data from two sites from the Castlegate Sandstone and four from the Neslen Formation (Figs. 2, 3A) in eastern Utah, from the upper part of the Castlegate Sandstone and the lower and middle parts of the Neslen Formation. From the six principal study localities, sixty-two graphic logs were measured that record lithology, bed thickness, grain size, sedimentary structures, occurrence of fossils and palaeosols. Physical correlation of prominent beds and bounding surfaces between each measured graphic log was undertaken to establish geometrical relationships between individual crevasse-splay architectural elements, adjacent channel elements and other distal floodplain elements (Fig. 3C). Tracing beds permitted construction of 27 architectural panels and photomosaics across the studied sections. These record lateral changes of both the internal lithofacies organisation of splay elements, and the external geometry of the splay elements. In total, 1118 palaeocurrent measurements from cross-bedding foresets, ripple cross-lamination, ripple-forms on bedding surfaces and low-angle-inclined accretion surfaces are used to identify dip and strike sections of the studied crevasse-splay elements. This permits lengths, widths and thicknesses of the preserved crevasse-splay elements and their facies belts to be determined (Fig. 3D). Strike sections are defined as 0-30 degrees from the outcrop orientation, oblique as 30-60 degrees from outcrop orientation and dip sections as 60-90 degrees from outcrop orientation. Full lengths and widths of splays are calculated from partial exposures using thinning rates within the window of outcrop of observation.

The collation of each of these data types has allowed identification and quantification of lateral and vertical changes in facies type within 35 individual splay bodies, of which 20 have been dip- and strike-corrected to determine original widths and lengths. For splay bodies characterised internally by facies that yield palaeocurrent information, and which were laterally more extensive than the outcrop, the predicted minimum size of the splay element was determined using element thinning rates in the known direction of growth. Thinning rates were used to extrapolate, in the direction of main palaeoflow, down to zero to produce the predicted length of the splay. This method allows quantitative analysis of the dimensions and stratigraphic changes in splay proportion in overbank successions.

A 40 m-thick interval within the Lower Neslen Formation exposed in a 1.5 km-long cliff-face in Tuscher Canyon to the east of Green River (Fig. 3C) has been chosen as a type succession. Here, a 20 m thick, 1.5km long, detailed architectural panel has been constructed from 11 measured graphic logs, which collectively total 315 m in measured thickness. Two marker beds that are present continuously constrain the studied stratigraphic interval: a shell bed at the boundary between the Sego Sandstone and base of the overlying Neslen Formation, and a laterally extensive coal seam (Fig. 5).

Through high-resolution chronostratigraphic correlation the sedimentary architecture has been reconstructed to show how crevasse-splay deposits contribute to the construction of an overbank succession (Fig. 5).

5. Lithofacies

Eleven lithofacies types are recognised based on composition, grain size, sediment textural characteristics and sedimentary structures (Figs. 4, 5; Table 1). The facies scheme is an extended version of the schemes of Miall (1985) and Colombera et al. (2013).

6. Architectural characteristics of crevasse-splay bodies

Three architectural-element types are identified: crevasse-channel, crevasse-splay and coal-prone floodplain elements. Each element type is composed internally of distinctive lithofacies associations that are vertically and laterally distributed in a repeatable pattern with distinct geometrical properties that are discernible from those of non-diagnostic overbank deposits. Relationships both within and between these elements have been traced out laterally, i.e., walked out (Fig. 5), to define a predictable succession of lateral facies transitions from the proximal (relative to the parent channel element to which the splay body is likely genetically linked), through medial and distal parts of splay bodies to adjoining floodplain deposits. Through establishment of empirical relationships, the length scale of facies transitions within individual splay elements can be used to predict distance to parent feeder channel (Fig. 6A).

Crevasse-channel elements

Crevasse-channel elements are channel forms with a basal surface that truncates the underlying strata, typically proximal or medial splay elements. Crevasse-channel elements are well exposed at the Tuscher Canyon and Floy Canyon sites in the Neslen Formation (Fig. 7A). Planar-cross bedded sandstone (St/Sp) and ripple cross-laminated sandstone (Sr) are the most dominant facies in this element (Fig. 6C). Crevasse-channel-fills have an average thickness of 1.4 m (0.6 m to 2.4 m, n = 5) (Fig. 6B) and have lenticular geometries in cross section (Fig. 6A). Commonly the channel-fills have sharp or erosional top surfaces but can have gradational tops where they pass into overlying fine-grained facies of non-diagnostic overbank origin.

Associations of facies are commonly arranged vertically as successions of planar cross-bedded sandstone (St/Sp) overlain by thin (<0.5 m) sets of ripple cross-laminated sandstone (Sr), ripple cross-laminated sandstones (Sr), and soft-sediment deformed chaotic sandstone and siltstone, all capped by structureless siltstones (Fp/op). Alternatively, sets of soft-sediment deformed chaotic sandstone and siltstone (Fd) may be capped by thin (<0.7 m) sets of structureless poorly sorted siltstone (Fp) (Fig. 7A).

Sandstone-prone crevasse-channel elements indicate a close proximity to the flood-breach; farther away from the breach, the more silt-prone facies indicate gradual deceleration and overfilling of crevasse channels with fines.

Splay elements

Proximal facies belt

The proximal facies belts of splay elements are composed internally of the following facies associations: trough and planar cross-bedded sandstones (St/Sp), structureless sandstone (Sm), ripple cross-laminated sandstone (Sr), soft-sediment deformed chaotic sandstone and siltstone (Fd) and poorly sorted siltstone (Fp) (Fig. 6A, 6C). Commonly, proximal splay elements exhibit the coarsest grain size (up to upper-fine sandstone; average fine sandstone) of the entire overbank succession (Fig. 6A, 6C), and the greatest overall thicknesses (Fig. 6B): up to 3.7 m. Structureless sandstone (Sm) and ripple cross-laminated sandstones (Sr) are the dominant facies of proximal splays elements (Fig. 6C).

The proximal facies belts of splay elements exhibit wedge or tabular geometries (Fig. 6A) and have an average thickness of 2.1 m (1.0 to 3.7 m) (n = 27 measured occurrences of 35 studied splay bodies) (Fig. 6B). Mean lateral dip-section extent is 129 m (55 to 189 m) (n= 8); strike sections of the proximal facies belt have a mean extent of 278 m (75 to 676 m) (n= 10) (Fig. 9D). These bodies have sharp tops and sharp but mostly non-erosional bases, though with rare gutter casts (<0.5 m wide) (Fig. 5; Logs 1-3 at 23 m).

The proximal facies belts of splay elements may also exhibit different vertical arrangements of lithofacies: sets of structureless sandstone (Sm) are commonly overlain either by rippled sandstone (Sr; <0.4 m) or thin, poorly sorted siltstone (Fp; <0.4 m). Sets of rippled sandstone (Sr) can be overlain by thin (<0.4 m) structureless sandstone and siltstone (Fd), or by poorly sorted siltstone (Fp). Sets of planar cross-bedded sandstone (St/Sp) can be overlain by rippled sandstones (Sr) (Fig. 7B). The most common configuration is Sm and Fp, or St/Sp and Sr, and Sr alone is also common (comprising 15 to 55% of each studied vertical succession) (Fig. 7B).

Parts of splay elements defined as proximal show variable internal facies arrangements that suggest variations in flood energy during deposition. The facies arrangement consisting of St/Sp topped with Fp, and Sm topped with Fp, represents the preserved expression of a downstream waning flow during splay flood events. Other trends, notably Sm topped by Sr, and the lack of preserved genetically related fine-grained caps indicate (i) that the subsequent reduction in flow energy could have occurred suddenly, (ii) that fine-grained sediment fractions were bypassed to more distal parts of the system, or (iii) that subsequent flows eroded fine-grained caps. In this instance, we interpret that absence of caps indicate that the flow across the splay transported finer-grained sediment fractions farther into the floodbasin.

Medial facies belt

The proximal part of a splay element thins and fines gradationally into the medial facies belt of the splay element. Medial deposits are differentiated from more proximal deposits by their finer grain size (medium siltstone to fine sandstone; average very-fine sandstone), the overall reduction in the occurrence of sedimentary structures such as ripple strata, and the increased occurrence of soft-sediment deformation features (Fig. 6A, 6C). Medial splay deposits comprise structureless sandstone (Sm), small-scale ripple cross-laminated sandstone (Sr), soft-sediment deformed sandstone with remnant ripple forms (Sr), soft-sediment deformed chaotic sandstone and siltstone (Fd), and structureless poorly-sorted siltstone (Fp/Fop). Facies Sr and Fd are the dominant facies types recorded in this element, comprising 20.3% and 43%, of medial splay elements, respectively (Fig. 6C).

The medial parts of splay elements have an average thickness of 1.5 m (0.2 to 2.6 m) (n = 63 measured occurrences in 35 studied splay bodies) (Fig. 6B) and extend laterally in dip section for an average of 204 m (124 to 281 m) (n = 4) (Fig. 6A) and in strike section for 423 m (112 to 848 m) (n = 10) (Fig. 9D); they exhibit tabular to wedge-like geometries (Fig. 6A). The basal surfaces of these elements are sharp; gutter casts are much less common than in proximal parts of splay elements.

Typical vertical arrangements of lithofacies in medial facies belt are thin sets of rippled sandstone (Sr) (<0.5 m) overlain by soft-sediment deformed chaotic sandstone and siltstone (Fd), and poorly sorted siltstone (Fp/op) (Fig 7C). Soft-sediment deformed sandstone with remnant ripple-forms (Sr) and soft-sediment deformed chaotic sandstone and siltstone (Fd) can both occur alone (Fig. 7C). At every site where medial parts of the splay are recorded facies arrangements contain Sr facies; the association of facies Sr and Fd, Sr and Fp, or Sr alone characterize 30% to 50% of facies types recorded in each medial splay element (Fig. 7C). Each vertical arrangement of facies tends to show either a fining-upwards trend or no discernible grain-size trend (Fig. 7C). Examples of medial facies belts in both the Castlegate Sandstone and the Neslen Formation are similar. However, associations of facies Sr and Fd are not noted in the Castlegate Sandstone, whereas associations of facies Sr and Fp are abundant (Fig. 7C). The occurrence of deformed facies Sd and Fd within such medial splay elements implies rapid sediment accumulation on a water-saturated substrate that induced soft-sediment deformation (Rossetti and Santos, 2003; Owen and Santos, 2014). There is little discernible difference in the form of medial splay elements within the Castlegate and the Neslen formations (Fig. 7C).

Distal facies belt

The medial facies belt thins and fines, and laterally passes into the distal facies belt, which is itself characterized by a finer modal grain size (fine siltstone to very-fine sandstone; on average medium siltstone), a further reduction in the occurrence of primary sedimentary structures, no convolute lamination or ripples, and by draping or flat set geometries (Fig. 6A). Distal parts of splay elements comprise soft-sediment deformed chaotic sandstone and siltstone (Fd), structureless poorly sorted rooted siltstone (Fp) and structureless organic-rich poorly sorted siltstone (Fop) (Fig. 6C). Structureless poorly sorted rooted siltstone (Fp) and structureless organic-rich poorly sorted siltstone (Fop) are the most common facies, comprising 60.1% and

25.6%, of the facies types recorded distal facies belts, respectively (Fig. 6C). Distal parts of splay elements have an average bed thickness of 0.8 m (0.2 to 1.6 m) (n = 57 occurrences of 35 studied splay bodies), extend laterally in dip-section for an average of 229 m (118 to 286 m) (n = 2) and in strike section for 399 m (113 to 852 m) (n = 7) (Fig. 9D), and show tabular geometries (Fig. 6A). The basal surfaces of these elements are sharp but non-erosional. Distal facies belts comprise a predictable vertical succession of facies: thin (<0.5 m) soft-sediment deformed chaotic sandstone and siltstone (Fd) topped with poorly sorted siltstone (Fp/op) or, more commonly, structureless poorly sorted siltstone (Fp/op) alone (Fig. 7D).

Soft-sediment deformed chaotic sandstone and siltstones (Fd) topped with structureless poorly sorted siltstones are present in many studied examples of distal splay elements but are particularly common in examples from Crescent Canyon (making up 55% of the overbank succession at this locality). Generally, the Castlegate Sandstone exhibits more structureless organic-rich poorly sorted siltstones (Fop) than the Neslen Formation (Fig. 7D). The organic matter content could be due to local variations in floodplain vegetation type or abundance, or due to variation in the frequency of occurrence of floodwaters capable of incorporating organic matter into the flow, which itself might be due to local hydrodynamic conditions that favour accumulation of organic matter (Morozova and Smith, 2003).

Coal-prone floodplain element

Typically, the distal part of a splay element is laterally juxtaposed by coal-prone floodplain elements. Locally, distal splay elements merge gradationally with floodplain elements. Coal-prone floodplain elements are the finest grained elements in the overbank and comprise: laminated organic-rich siltstones (Fl), laminated rooted siltstones (Fr) and coals (C) (Fig. 6A). Laminated organic-rich siltstones (Fl) are the most common facies in the floodplain (84%) (Fig. 6C).

Coal-prone floodplain elements have an average thickness of 0.6 m (0.2 to 1.6 m) (Fig. 6B). Element bases can be sharp or gradational; geometries tend to be tabular and laterally extensive (Fig. 6B).

Coals are more common in the lower Neslen Formation. Laminated organic-rich siltstones (Fl) is dominant through all sites (Fig. 7E) while laminated rooted siltstones are far less abundant, making up less than 20% of the overbank succession at every site (Fig. 7E). Sites that have slightly more rooted siltstones (Fr) tend to have lower coal (C) proportions (Fig. 7E). This suggests a localised change in drainage conditions to a well-drained environment, perhaps due to fluctuating water-table levels (Bown and Kraus, 1987).

Overbank succession

The identified architectural elements, each of which represents the preserved expression of a depositional sub-environment, make different proportions (based on logged thicknesses) of the overbank succession at each study locality in the Castlegate and Neslen formations (Fig. 8). However, these proportions may be biased since the studied outcrops were selectively chosen based on the occurrence of deposits that are interpretable as crevasse-splay elements, and so might not be representative of the studied fluvial successions as a whole. Crevasse-channel fills only occur at Tuscher Canyon and Floy (Fig 8).

The high-resolution stratigraphic tracing and correlation of individual crevasse-splay elements in this study has demonstrated that a significant proportion of overbank deposits represent the distal parts of splay elements (19.8% in the Castlegate Sandstone; 22.5% in the Neslen Formation) (Fig. 8). Compared to the distal parts of crevasse-splay bodies, the floodplain fines comprise a similar amount of the overbank (29.6% in the Castlegate Sandstone; 24.3% in the Neslen Formation) (Figs. 8, 10).

The panel depicting the sedimentary architecture at Tuscher Canyon (Fig. 5) demonstrates how the various architectural elements and facies belts combine to form a succession. The splay elements commonly incise the upper part of the underlying finer-grained floodplain element (Fig. 5C). Medial and distal parts of the crevasse-splay bodies interfinger with laminated fines of floodplain elements (Fig. 5D). Although superficially similar, the lithofacies types present in these sub-environments are distinct (Table 1).

7. Discussion

Quantification of splay dimensions

Lithofacies and architectural element analysis has allowed for the development of a predictive facies model for the studied successions, which are characterized by preserved remnants of crevasse-splay deposits. The architectural elements of the crevasse-splay deposits comprise a significant proportion of the overbank as a whole: average 60% of the Castlegate Sandstone overbank and 69% of the Neslen Formation overbank successions (Fig. 10). The documented crevasse-splay elements have an average length of 544 m (observed range is 292 to 750 m) (n = 8), an average width of 1040 m (observed range is 300 to 1503 m) (n = 12), and an average preserved thickness of 1.7 m (observed range is 0.6 to 2.6 m) (Figs. 6, 9). Length and width values include apparent and incomplete measurements for which true extents cannot be determined (cf., Greehan and Underwood, 1993). These dimensions are here used to estimate splay volume, whereby splay elements are approximated as flat-based radial bodies with a domed upper surface that approximates in shape to a quarter of a flattened ellipsoid (Fig. 9):

$$0.25\left(\frac{4}{3}\pi\ L\ t\frac{1}{2}W\right)$$

where L is the length, W the width and t the thickness (Fig. 9). Using this approximation, the average calculated volume for an individual crevasse-splay body is 5.036×10^{5} m^3 (n = 20). A Pearson product-moment correlation coefficient to assess the relationship between maximum recorded thickness and splay length yields an r-value of 0.26, indicating a weak correlation and a p-value of <0.01, indicating significance of the relationship (Fig. 3, 9C). The lengths of the splay bodies recorded herein are less than the overall widths, but are comparable to the half widths (W/2) (Fig. 9C, 9D) (cf., Zwolinski, 1991; Miall, 1994). The addition of literature-derived data (Table 2) to splay length data from this study yields a Pearson r-value of 0.70 and a p-value of <0.001 (Fig. 9C), and demonstrates a strong relationship between splay thickness and splay lengths. The maximum preserved splay element thickness in a vertical section is an indicator of the overall size (length and width) of a splay body.

Mjøs et al. (1993) and van Toorenenburg et al. (2016) present ancient splay body volumes that are larger (10^8 m^3 and 10^7 m^3, respectively). These larger values could arise because the splays studied by these authors were generated by larger rivers in floodbasins with more accommodation, or were vertically or laterally amalgamated (composite). In addition, the average volume presented herein might represent an underestimation, in relation to the inclusion of apparent and incomplete measurements. Also, the definitions of splay limits used in these studies could have differed from those used here, and different calculations with different inherent biases could have been used in the other studies.

Controls on crevasse-splay size

The dimensions of splay bodies examined in this study lie in the middle of the range of values recorded from other studies (Table 2). Controls that could account for variations in the size and shape of studied crevasse-splay bodies when compared to published studies include: (i) formative channel size; (ii) style of lateral and vertical amalgamation of splays; (iii) availability and shape of floodbasin accommodation; and (iv) gradient from the point of levee breach to floodbasin floor.

The formative parent-channel size partly determines the associated splay-body size; larger channels tend to experience larger floods and thereby generate larger associated crevasse splays (Table 2). The size of a splay body will also, in part, depend on whether it is possible to distinguish between an individual splay body versus a composite element formed from multiple amalgamated splay bodies. Lateral and vertical amalgamation of individual splay elements can result in deposits of greater thickness. Factors such as proximity to other splay bodies in a floodbasin, the repeat frequency of splay development at a particular site, and the amount of incision associated with splay emplacement over older splay deposits, will influence the amount of lateral or vertical amalgamation of splay deposits. Vertical amalgamation occurs where several crevasse-splay deposits stack together, with younger deposits potentially partly eroding older deposits (e.g., Fig. 5C). Such vertical amalgamation results in the generation of thicker crevasse-splay stacks that might represent composite flood events, possibly associated with sand-on-sand contacts (van Toorenenburg et al., 2016). Lateral stacking and amalgamation occur where younger or time-equivalent crevasse-splay bodies partially overlap older or time-equivalent crevasse-splay bodies

(Li et al., 2014). This can occur where the sand-prone, proximal parts of two crevasse splays merge to create a sand-on-sand contact (van Toorenenburg et al., 2016), or where the silt-prone, distal parts of two crevasse-splay bodies merge (Fig. 5D).

The availability and spatial extent of floodbasin accommodation, and the possible presence of positive relief features in the floodbasin are important controls that influence crevasse-splay size and shape. Features such as older splay deposits (Li et al., 2015), or raised mires on the floodplain (Perez-Arlucea and Smith, 1999) will influence splay-deposit size and shape. It might be expected that the size of splay deposits will scale directly to the amount of available accommodation (negative relief). Therefore, the thickness of the preserved splay deposit can be used as an indicator for minimum accommodation on the floodplain at the time of deposition. Specifically, in the overbank successions studied in the Castlegate Sandstone and the Neslen Formation, there is an abundance of organic-rich siltstones and coal beds (Fig. 8), which have greater compaction factors (Nadon, 1998) and could act as a generator for floodplain accommodation (Franczyk, 1990; Hettinger and Kirschbaum, 2003; Shiers et al., 2014; 2017). In turn, although the organic-rich siltstones and coal beds can produce additional accommodation via autocompaction, they could not have formed initially without space being available on the floodplain.

Fluctuations in floodbasin gradient can encourage crevasse-splay deposition, with deposition likely preferentially occurring in areas where the gradient decreases between proximal and distal reaches of the floodbasin (cf., Adams et al., 2004). Studied splay elements exhibit an average rate of thinning of 4.60×10^{-3} m/m in the width orientation (w/2) and 3.37×10^{-3} m/m in the length orientation.

Controls on the length scale of facies belts within crevasse-splay elements

The proximal to distal fining within splay bodies reflects a general down-current decrease in flow depth, velocity and sediment concentration as the flood waters expand and spread across the floodbasin (Bridge, 1984; Miall, 1993; Smith and Perez-Arlucea, 1994; Bristow, 1999; Anderson, 2005; Fisher et al., 2008) (Figs. 6A, 10). Furthermore, discharge decreases distally due to transmission losses.

The proximal sandstone-prone parts of splays are less dominant than the finer-grained, silt-prone medial and distal parts. Within the successions studied here, the proximal splay belt comprises on average 25% (15 to 47%) of the splay body volume, the medial 37% (22 to 56%) and the distal 38% (18 to 63%). Any variations in the lateral extent of the facies transitions (Fig. 9B) most likely reflects facies belts in the preserved splay element that are irregular in geometry (cf. Nichols and Fisher, 2007; Fisher et al., 2008; Cain and Mountney, 2009) (Fig. 10).

Sediment calibre, which governs how sediment is carried in the flow (bedload or suspended load), affects both extent and shape of facies belts within splay deposits, and the sedimentary structures that develop. Each part of the splay body exhibits a different association of facies (Fig. 6C). The dominant facies types in the most proximal reaches is Sm 31% deposited from suspension and Sr 49% dominantly bedload tractional deposit (Fig. 6C). . In the more medial and distal reaches, Fd 59% (Fig 6.C medial portion) and Fp 53% (Fig. 6C distal portion) are deposited predominantly from suspension. During flood events, the sand-grade sediment fraction carried as bedload is deposited preferentially in the proximal part of the splay, whereas the silt and clay fraction is transported in suspension to be deposited in more distal parts of the splay where flow rates are reduced.

The overall sediment grain-size distribution of the material supplied by the parent river to the splay exerts a fundamental control on the length-scale of facies belts present in a single splay body. Flows that carry a greater proportion of sand tend to be characterised by laterally more extensive proximal facies belts. Fluvial systems with main channels that carry a significant volume of sand in suspension will favour the development of relatively more sand-prone splays.

The occurrence of crevasse-splay elements in overbank successions

The finer portions of crevasse-splay elements and the sediment deposited from suspension in fluvial floodbasin, i.e., finer-grained floodplain elements, can look superficially similar. However, the high-resolution stratigraphic correlation of individual crevasse-splay elements in this study demonstrate that a significant proportion of non-channelized deposits represent the distal parts of splay elements

(19.8% on average in the Castlegate Sandstone; 22.5% on average in the Neslen Formation) (Fig. 8). The floodplain fines comprise a similar amount of the overall overbank as the distal parts of crevasse splays (29.6% on average in the Castlegate Sandstone; 24.3% on average in the Neslen Formation), in the study areas (Figs. 8, 10).

Several possible controlling factors influence crevasse-splay occurrence and the preservation potential of accumulated splay elements: channel pattern, development of mires and base level changes. Meandering patterns as opposed to braided patterns tend to encourage splay deposition, with floodplain deposits proportionally making up very little of the overall preserved succession of braided systems (Bristow et al., 1999; Colombera et al., 2013). Rivers of the Neslen Formation have been interpreted to have been characterized by meandering channels of modest size (Franczyk et al., 1990; Kirschbaum and Hettinger, 2004; Shiers et al., 2014), which likely encouraged the occurrence of crevasse splays. Average point-bar thickness in bar deposits associated with the main channel elements of the Neslen formation are 7m thick. Average abandoned channel element widths are 80m (Shiers et al., 2017). Rivers with meandering patterns encourage flooding and crevassing due to the helical nature of the flow in sinuous rivers and the increased amount of overbank sediment flux towards the outer bank, especially during episodes of increased discharge (Ten Brinke et al., 1998), assuming that these splays are preserved and not cannibalised by the migrating channel. Conversely, raised mires can inhibit splay formation (Perez-Arlucea and Smith, 1999), through topographic relief that reduces or inverts the gradient difference between the parent channel and the floodplain or which stabilise channel banks. Both factors reduce the likelihood of splay development, or allow only laterally restricted and confined splay development. Base-level rise has been shown to play an important role in encouraging accumulation of crevasse-splay bodies with an increased rate of accommodation generation encouraging preservation of splay deposits (Zwolinski, 1991; Bristow et al., 1999). An increase in the occurrence of crevasse-splay and floodplain deposits is noted upwards through the Lower Nelsen Formation (Shiers et al., 2014), and this is likely due to the influence of a rising base level associated with a longer term transgressive systems tract (Kirschbaum and Hettinger, 2004; Shiers et al., in press).

Differentiating a crevasse-splay element from a fine-grained floodplain element in the rock record remains problematic. Floodplain mudstones mostly comprise suspension deposits accumulated in floodbasin or floodplain lake settings (Miall, 1994); however it is difficult to determine whether the route that such sediments take to reach these sites of accumulation is via levee overtopping or via crevassing. In outcrop, the distal parts of crevasse splays from the floodplain fines can only be discriminated by walking out splay elements (Fig. 5, log 5 to 6). Practically, this study has shown that the distinction should be facilitated by high-resolution facies and architectural-element analyses conducted with lateral tracing of bounding surfaces.

Conclusions

This study discusses the important role crevasse-splay deposits play in building overbank successions. Splay deposits in this study make up a significant component of the overbank: up to 90% in the studied outcrops (Fig. 8). High-resolution facies and architectural-element analyses of crevasse-splay deposits allow overbank successions to be described in terms of depositional sub-environments: crevasse channels, and proximal, medial and distal splay deposits. Associations of lithofacies define the internal subdivisions of splay bodies. Proximal parts of splays are significantly more sandstone-prone and are characterised by cross-lamination. By contrast distal parts of splays are siltstone-prone and structureless. Lithofacies associations are arranged into vertical and lateral successions that occur in predictable orders: cross-laminated sandstone sets pass laterally to deformed finer-grained sandstone sets, which themselves pass laterally to structureless siltstone sets. These lateral transitions occur across average length and width scales of ca. 500 m and ca. 1000 m (full width), respectively, resulting in a planform shape that is approximately elliptical rather than lobate-teardrop. Crevasse-channel elements, crevasse-splay elements with proximal, medial and distal facies belts, and coal-prone floodplain elements are each defined by a subtle internal arrangement of lithofacies. Such trends can be used to predict the occurrence and facies architecture of relatively more sand-prone or more silt-prone parts of the overbank. Within the studied overbank settings, coarser sandstone deposits occur solely in crevasse-channel and proximal splay elements; finer sandstone and siltstone deposits dominate in medial and distal splay elements; siltstone and coal-prone deposits characterize aggradational floodplain elements.

Because splay elements represent a larger proportion of the overbank succession than coal-prone floodplain elements in the studied successions, the internal complexity of splay deposits presented in this paper takes on more importance when investigating potential reservoirs in low net-to-gross fluvial settings.

Acknowledgements

This research was funded by Areva, BHPBilliton, ConocoPhillips, Det norske oljeselskap ASA (Detnor), Murphy Oil Corporation, Nexen-CNOOC, Saudi Aramco, Shell, Tullow Oil, Woodside, and YPF, through their sponsorship of the Fluvial & Eolian Research Group. LC is supported by NERC (Catalyst Fund award NE/M007324/1; Follow-on Fund NE/N017218/1). Kate Melbourne and Josh Khan are thanked for their assistance with field data collection. Michelle Shiers, Richard Collier and Catherine Russell are thanked for their help and advice.

References

Adams, P.N., Slingerland, R.L., Smith, N.D., 2004. Variations in natural levee morphology in anastomosed channel flood plain complexes. Geomorphology 61, 127-142.

Adams, M., Bhattacharya, J.P., 2005. No change in fluvial style across a sequence boundary, Cretaceous Blackhawk and Castlegate Sandstones of central Utah, USA. Journal of Sedimentary Research 75, 1038-1051.

Allen, J.R., 1963. The classification of cross-stratified units with notes on their origin. Sedimentology 2, 93-114.

Allen, J., 1977. The possible mechanics of convolute lamination in graded sand beds. Journal of the Geological Society 134, 19-31.

Anderson, D.S., 2005. Architecture of Crevasse Splay and Point-Bar Bodies of the Nonmarine Iles Formation north of Rangely, Colorado: Implications for Reservoir Description. The Mountain Geologist, 42, 109-122.

Arnaud-Fassetta, G., 2013. Dyke breaching and crevasse-splay sedimentary sequences of the Rhône Delta, France, caused by extreme river-flood of December 2003. Geografia Fisica e Dinamica Quaternaria 36, 7-26.

Arndorfer, D.J., 1973. Discharge patterns in two crevasses of the Mississippi River delta. Marine Geology 15, 269-287.

Aschoff, J., Steel, R., 2011. Anomalous clastic wedge development during the Sevier-Laramide transition, North American Cordilleran foreland basin, USA. Geological Society of America Bulletin 123, 1822-1835.

Aschoff, J.L., Steel, R.J., 2011. Anatomy and development of a low-accommodation clastic wedge, upper Cretaceous, Cordilleran Foreland Basin, USA. Sedimentary Geology 236, 1-24.

Baeteman, C., Beets, D.J., Van Strydonck, M., 1999. Tidal crevasse splays as the cause of rapid changes in the rate of aggradation in the Holocene tidal deposits of the Belgian Coastal Plain. Quaternary International 56, 3-13.

Behrensmeyer, A.K., Willis, B.J., Quade, J., 1995. Floodplains and palaeosols of Pakistan Neogene and Wyoming Palaeogene deposits: a comparative study. Palaeogeography, Palaeoclimatology, Palaeoecology 115, 37-60.

Bown, T.M., Kraus, M.J., 1987. Integration of channel and floodplain suites, I. Developmental sequence and lateral relations of alluvial palaeosols. Journal of Sedimentary Petrology 57, 587-601.

Bridge, J.S., 1984. Large-scale facies sequences in alluvial overbank environments. Journal of Sedimentary Research 54, 85-170.

Bridge, J.S., 2006. Fluvial facies models: recent developments. In: Posamentier, H.W., Walker, R.G. (Eds.), Facies Models Revisited. SEPM Special Publication 84, pp. 85–117.

Bridge, J.S., Demicco, R.V., 2008. Earth Surface Processes, Landforms and Sediment Deposits. Cambridge University Press, Cambridge,815 pp.

Brierley, G.J., Hickin, E.J., 1992. Floodplain development based on selective preservation of sediments, Squamish River, British Columbia. Geomorphology 4, 381-391.

Brierley, G.J., Ferguson, R.J., Woolfe, K.J., 1997. What is a fluvial levee? Sedimentary Geology 114, 1-9.

Bristow, C., Skelly, R., Ethridge, F., 1999. Crevasse splays from the rapidly aggrading, sand-bed, braided Niobrara River, Nebraska: effect of base-level rise. Sedimentology 46, 1029-1048.

Buehler, H.A., Weissmann, G.S., Scuderi, L.A., Hartley, A.J., 2011. Spatial and temporal evolution of an avulsion on the Taquari River distributive fluvial system from satellite image analysis. Journal of Sedimentary Research 81, 630-640.

Cahoon, D.R., White, D.A., Lynch, J.C., 2011. Sediment infilling and wetland formation dynamics in an active crevasse splay of the Mississippi River delta. Geomorphology 131, 57-68.

Cain, S.A., Mountney, N.P., 2009. Spatial and temporal evolution of a terminal fluvial fan system: the Permian Organ Rock Formation, South-east Utah, USA. Sedimentology 56, 1774-1800.

Cloyd, K.C., Demicco, R.V., Spencer, R.J., 1990. Tidal channel, levee, and crevasse-splay deposits from a Cambrian tidal channel system: a new mechanism to produce shallowing-upward sequences. Journal of Sedimentary Petrology 60, 73-83.

Cole, R., 2008. Characterization of fluvial sand bodies in the Neslen and lower Farrer formations (Upper Cretaceous), Lower Sego Canyon, Utah. In: Longman, M.W., Morgan, C.D. (Eds.), Hydrocarbons Systems and Production in the Uinta Basin, Utah. Rocky 14 Mountain Association of Geologists—Utah Geological Association Publication, 37, pp. 81–100.

Coleman, J.M., 1969. Brahmaputra River: Channel processes and Sedimentation Brahmaputra River: Channel processes and sedimentation. Sedimentary Geology 3, 129-239.

Collinson, J.D., Mountney, N., Thompson, D., 2006. Sedimentary Structures, third edition. Terra Publishing, Hertfordshire, England.

Colombera, L., Felletti, F., Mountney, N.P., McCaffrey, W.D., 2012. A database approach for constraining stochastic simulations of the sedimentary heterogeneity of fluvial reservoirs. AAPG Bulletin 96, 2143-2166.

Colombera, L., Mountney, N.P., McCaffrey, W.D., 2013. A quantitative approach to fluvial facies models: Methods and example results. Sedimentology 60, 1526-1558.

Colombera, L., Shiers, M.N., Mountney, N.P., 2016. Assessment of backwater controls on the architecture of distributary-channel fills in a tide-influenced coastal-plain succession: Campanian Neslen Formation, U.S.A. Journal of Sedimentary Research 86, 1-22.

Farrell, K.M., 1987. Sedimentology and facies architecture of overbank deposits of the Mississippi River, False River region, Louisiana. In F.G. Ethridge, R.M. Flores, J.D. Harvey (Editors), Recent Developments in Fluvial Sedimentology. Spec. Publ. Soc. Econ. Paleont. Miner., vol 39, 111-120.

Farrell, K.M., 2001. Geomorphology, facies architecture, and high-resolution, non-marine sequence stratigraphy in avulsion deposits, Cumberland Marshes, Saskatchewan. Sedimentary Geology 139, 93-150.

Franczyk, K.J., Pitman, J.K., Nichols, D.J., 1990. Sedimentology, mineralogy, palynology, and depositional history of some uppermost Cretaceous and lowermost Tertiary rocks along the Utah Book and Roan Cliffs east of the Green River, US Government Printing Office. USGS Bulletin, 1-27.

Fisher, J.A., Krapf, C.B.E., Lang, S.C., Nichols, G.J., Payenberg, T.H.D., 2008. Sedimentology and architecture of the Douglas Creek terminal splay, Lake Eyre, central Australia. Sedimentology 55, 1915-1930.

Ghazi, S., Mountney, N.P., 2009. Facies and architectural element analysis of a meandering fluvial succession: the Permian Warchha Sandstone, Salt Range, Pakistan. Sedimentary Geology 221, 99-126.

Ghazi, S., Mountney, N.P., 2011. Petrography and provenance of the Early Permian fluvial Warchha Sandstone, Salt Range, Pakistan. Sedimentary Geology 233, 88-110.

Geehan, G., Underwood, J., 1993. The use of length distributions in geological modelling. In: Flint, S.S., Bryant, I.D. (Eds.), The Geological Modelling of Hydrocarbon Reservoirs and Outcrop Analogues. International Association of Sedimentologists Special Publication 15, pp.205-212.

Gugliotta, M., Flint, S.S., Hodgson, D.M., Veiga, G.D., 2015. Stratigraphic record of river-dominated crevasse subdeltas with tidal influence (Lajas Formation, Argentina). Journal of Sedimentary Research 85, 265-284.

Gulliford, A.R., Flint, S.S., Hodgson, D.M., 2014. Testing applicability of models of distributive fluvial systems or trunk rivers in ephemeral systems: reconstructing 3-D fluvial architecture in the Beaufort Group, South Africa. Journal of Sedimentary Research 84, 1147–1169.

Hampson, G.J., Davies, W., Davies, S.J., Howell, J.A., Adamson, K.R., 2005. Use of spectral gamma-ray data to refine subsurface fluvial stratigraphy: late Cretaceous strata in the Book Cliffs, Utah, USA. Journal of the Geological Society 162, 603-621.

Hein, T., Baranyi, C., Herndl, G.J., Wanek, W., Schiemer, F., 2003. Allochthonous and autochthonous particulate organic matter in floodplains of the River Danube: the importance of hydrological connectivity. Freshwater Biology 48, 220-232.

Hettinger, R.D., Kirschbaum, M.A., 2002. Stratigraphy of the Upper Cretaceous Mancos Shale (upper part) and Mesaverde Group in the southern part of the Uinta and Piceance basins, Utah and Colorado, US Geological Survey. Pamphlet to accompany geologic investigations series i–2764.

Hettinger, R.D., Kirshbaum, M.A., 2003. Stratigraphy of the Upper Cretaceous Mancos Shale (Upper Part) and Mesaverde Group in the Southern Part of the Uinta and Piceance Basins, Utah and Colorado. USGS Uinta-Piceance Assessment Team, Comp., Petroleum Systems and Geologic Assessment of Oil and Gas in the Uinta-Piceance Province, Utah and Colorado. U.S. Geological Survey Digital Data Series DDS-69-B, pp. 1–16 .

Hornung, J., Aigner, T., 1999. Reservoir and aquifer characterization of fluvial architectural elements: Stubensandstein, Upper Triassic, southwest Germany. Sedimentary Geology 129, 215-280.

Jones, H., Hajek, E., 2007. Characterizing avulsion stratigraphy in ancient alluvial deposits. Sedimentary Geology 202, 124-137.

Jones, L.S., Harper, J.T., 1998. Channel avulsions and related processes, and large-scale sedimentation patterns since 1875, Rio Grande, San Luis Valley, Colorado. Geological Society of America Bulletin 110, 411-421.

Jones B.G., Rust B.R., 1983. Massive sandstone facies in the Hawkesbury sandstone, a Triassic fluvial deposit near Sydney, Australia. Journal of Sedimentary Petrology 53, 1249-1259.

Keeton, G.I., Pranter, M.J., Cole, R.D., Edmund, R., 2015. Stratigraphic architecture of fluvial deposits from borehole images, spectral-gamma-ray response, and outcrop analogs, Piceance Basin, Colorado. AAPG Bulletin 99, 1929-1956.

Keller, E.A., Swanson, F.J., 1979. Effects of large organic material on channel form and fluvial processes. Earth Surface Processes 4, 361-380.

Kirschbaum, M.A., Hettinger, R.D., 2004. Facies analysis and sequence stratigraphic framework of Upper Campanian Strata (Neslen and Mount Garfield Formations, Bluecastle Tongue of the Castlegate Sandstone, and Mancos Shale), Eastern Book Cliffs, Colorado and Utah. U.S. Geological Survey, U.S. Geological Survey Digital Data Report DDS-69-G

Kraus, M.J., 1999. Palaeosols in clastic sedimentary rocks: their geologic applications. Earth-Science Reviews 47, 41-70.

Li, J., Donselaar, M.E., Hosseini Aria, S.E., Koenders, R. Oyen A.M., 2014. Landsat imagery-based visualization of the geomorphological development at the terminus of a dryland river system. Quaternary International 352, 100-110.

Li, J., Bristow, C.S., 2015. Crevasse splay morphodynamics in a dryland river terminus: Río Colorado in Salar de Uyuni Bolivia. Quaternary International 377, 71-82.

Mack, G.H., James, W.C., Monger, H.C., 1993. Classification of palaeosols. Geological Society of America Bulletin 105, 129-136.

Marconato, A., De Almeida, R.P., Turra, B.B., Fragoso-Cesar, A.R.D.S., 2014. Pre-vegetation fluvial floodplains and channel-belts in the Late Neoproterozoic–Cambrian Santa Bárbara group (Southern Brazil). Sedimentary Geology 300, 49-61.

McCabe, P.J., 1987. Facies studies of coal and coal-bearing strata. In: Scott, A.C. (Ed.), Coal and Coal-bearing Strata: Recent Advances. Geological Society of London, Special Publications pp.32, 51-66.

McLaurin, B.T., Steel, R.J., 2007. Architecture and origin of an amalgamated fluvial sheet sand, lower Castlegate Sandstone, Book Cliffs, and Utah. Sedimentary Geology 197, 291-311.

Miall, A.D., 1985. Architectural-element analysis: a new method of facies analysis applied to fluvial deposits. Earth-Science Reviews 22, 261–308.

Miall, A.D., 1988. Facies architecture in clastic sedimentary basins. In: Kleinspehn, K., Paola, C. (Eds.), New Perspectives in Basin Analysis. Springer, Berlin-Heilderberg, New York, pp.67–81.

Miall, A.D., 1993. The architecture of fluvial-deltaic sequences in the upper Mesaverde Group (Upper Cretaceous), Book Cliffs, Utah. In: Best, J.L., Bristow, C. (Eds.), Braided Rivers. Geological Society of London, Special Publications 75, pp.305-332.

Miall, A.D., 1996. The Geology of Fluvial Deposits. Springer, Berlin.

Miall, A.D., 2014. Fluvial Depositional Systems, Springer, Berlin.

Miller, M., McCave, I., Komar, P., 1977. Threshold of sediment motion under unidirectional currents. Sedimentology 24, 507-527.

Mjøs, R., Walderhaug, O., Prestholm, E., 1993. Crevasse splay sandstone geometries in the Middle Jurassic Ravenscar Group of Yorkshire, UK. In: Marzo, M., Puigdefabregas, C. (Eds), Alluvial Sedimentation. International Association of Sedimentologists, Special Publication 17, pp.167-184.

Mohrig, D., Heller, P.L., Paola, C., Lyons, W.J, 2000. Interpreting avulsion process from ancient alluvial sequences: Guadalope-Matarranya system (northern Spain) and Wasatch Formation (western Colorado). Geological Society of America Bulletin 112, 1787-1803.

Morozova, G.S., Smith, N.D., 2003. Organic matter deposition in the Saskatchewan River floodplain (Cumberland Marshes, Canada): effects of progradational avulsions. Sedimentary Geology 157, 15-29.

Morris, E.A., Hodgson, D.M., Flint, S.S., Brunt, R.L., Butterworth, P.J., Verhaeghe, J., 2014. Sedimentology, Stratigraphic Architecture, and Depositional Context of Submarine Frontal-Lobe Complexes. Journal of Sedimentary Research 84, 763-780.

Nadon, G.C., 1998. Magnitude and timing of peat-to-coal compaction. Geology 26, 727-730.

Nanson, G., Croke, J., 1992. A genetic classification of floodplains. Geomorphology 4, 459-486.

Nichols, G.J., Fisher, J.A., 2007. Processes, facies and architecture of fluvial distributary system deposits. Sedimentary Geology 195, 75-90.

O'Brien, P., Wells, A., 1986. A small, alluvial crevasse splay. Journal of Sedimentary Petrology 56, 876-879.

Olsen, T., Steel, R., Hogseth, K., Skar, T., Roe, S.L., 1995. Sequential architecture in a fluvial succession: sequence stratigraphy in the Upper Cretaceous Mesaverde Group, Price Canyon, Utah. Journal of Sedimentary Research, Section B: Stratigraphy and Global Studies 65B, pp. 265-280.

Owen, G., 1978. Deformation processes in unconsolidated sands. In: Jones, M.E., Preston R.M.F. (Eds), Deformation of sediments and sedimentary rocks. Geological Society of London Special Publications 29, pp.11-24.

Owen, G., 1996. Experimental soft-sediment deformation: structures formed by the liquefaction of unconsolidated sands and some ancient examples. Sedimentology 43, 279-293.

Owen, G., Santos, M.G., 2014. Soft-sediment deformation in a pre-vegetation river system: the Neoproterozoic Torridonian of NW Scotland. Proceedings of the Geologists' Association 125, 511-523

Perez-Arlucea, M., Smith, N.D., 1999. Depositional patterns following the 1870s avulsion of the Saskatchewan River (Cumberland marshes, Saskatchewan, Canada). Journal of Sedimentary Research 69, 62-73.

Platt, N.H., Keller, B., 1992. Distal alluvial deposits in a foreland basin setting—the Lower Freshwater Miocene), Switzerland: sedimentology, architecture and palaeosols. Sedimentology 39, 545-565.

Retallack, G.J., 1988. Field recognition of palaeosols. Geological Society of America Special Papers 216, 1-20.

Rossetti, D.F., Santos, A.E., 2003. Events of sediment deformation and mass failure in Upper Cretaceous estuarine deposits (Cametá Basin, northern Brazil) as evidence for seismic activity. Sedimentary Geology 161, 107-130.

Rubin, D.M., 1987. Formation of scalloped cross-bedding without unsteady flows. Journal of Sedimentary Research 57, 39–45.

Shiers, M.S., Mountney, N.P., Hodgson, D.M., Cobain, S.L., 2014. Depositional controls on tidally influenced fluvial successions, Neslen Formation, Utah, USA. Sedimentary Geology 311, 1-16.

Shiers, M.S., Hodgson, D.M., Mountney, N.P., 2017. In press. Response of a coal-bearing coastal plain succession to marine transgression: Campanian Neslen Formation, Utah, U.S.A. Journal of Sedimentary Research, 87, xxx-xxx. DOI: http://dx.doi.org/10.2110/jsr.2017.7

Shiers, M.S., 2017. Controls on the deposition, accumulation and preservation of mixed fluvial and marginal-marine successions in coastal-plain settings. Unpublished PhD thesis, University of Leeds, Leeds.

Slingerland, R., Smith, N.D., 2004. River avulsions and their deposits. Annual Review of Earth and Planetary Sciences 32, 257–285.

Smith, N.D., Cross, T.A., Dufficy, J.P., Clough, S.R., 1989. Anatomy of an avulsion. Sedimentology 36, 1-23.

Smith, N.D., Perez-Arlucea, M., 1994. Fine-grained splay deposition in the avulsion belt of the lower Saskatchewan River, Canada. Journal of Sedimentary Research 64, 159-168.

Smith, N.D., Pérez-Arlucea, M., 2004. Effects of peat on the shapes of alluvial channels: examples from the Cumberland Marshes, Saskatchewan, Canada. Geomorphology 61, 323-335.

Staub, J.R., Cohen, A.D., 1979. The Snuggedy Swamp of South Carolina: a back-barrier estuarine coal-forming environment. Journal of Sedimentary Petrology 49, 133-143.

Ten Brinke, W., Schoor, M.M., Sorber, A.M., Berendsen, H.J., 1998. Overbank sand deposition in relation to transport volumes during large-magnitude floods in the Dutch sand-bed Rhine river system. Earth Surface Processes and Landforms 23, 809-824.

Toonen, W.H., Kleinhans, M.G., Cohen, K.M., 2012. Sedimentary architecture of abandoned channel fills. Earth Surface Processes and Landforms 37, 459-472.

Van Toorenenburg, K.A., Donselaar, M.E., Noordijk, N.A., Weltje, G.J., 2016. On the origin of crevasse-splay amalgamation in the Huesca fluvial fan (Ebro Basin, Spain): Implications for connectivity in low net-to-gross fluvial deposits. Sedimentary Geology 343, 156-164.

Van Wagoner, J.C., 1995. Sequence stratigraphy and marine to nonmarine facies architecture of foreland basin strata, Book Cliffs, Utah, and U.S.A. In: Van Wagoner, J.C., Bertram, G.T. (Eds.), Sequence Stratigraphy of Foreland Basin Deposits—Outcrop and Subsurface Examples from the Cretaceous of North America. AAPG Memoir 64, pp. 137–223.

Widera, M., 2016. Characteristics and origin of deformation structures within lignite seams–a case study from Polish opencast mines. Geological Quarterly 59, 181-19.

Willis, A., 2000. Tectonic control of nested sequence architecture in the Sego Sandstone, Neslen Formation and upper Castlegate Sandstone (Upper Cretaceous), Sevier foreland basin, Utah, USA. Sedimentary Geology 136, 277-317.

Zwoliński, Z., 1992. Sedimentology and geomorphology of overbank flows on meandering river floodplains. Geomorphology 4, 367-379.

Figure Captions

Figure 1. Schematic plan-view illustration of a typical crevasse-splay morphology. Thickness and grain size decrease away from the point source of the channel breach. (A) Plan-view schematic image of fluvial system with crevasse-splays. (B) Plan-view schematic image of a

crevasse-splay showing length and width orientations. (C) Cross-sectional view of width and lengths of crevasse-splay.

Figure 2. Stratigraphic scheme of the studied part of the Mesaverde Group, including the Castlegate and Neslen formations examined as part of this study. Based in part on Kirschbaum and Hettinger (2002) and Francyzk et al., (1991).

Figure 3. Location maps. (A) Location of Castlegate sites: Floy and Horse and Neslen sites: Tuscher, Tuscher 2, Crescent 3 and Crescent 4. (B) Representation of facies-belt regions of splays observed in the Castlegate and Neslen formations. Twenty splay elements composed of facies that yield palaeocurrent information were studied; the lines indicate the reconstructed orientations of the splay bodies based on analysis of palaeocurrent data with respect to outcrop orientation; the numbers indicate how many sections of each orientation have been recorded. (C) Tuscher Canyon cliff section; the position of each measured section is indicated.

Figure 4. Representative photographs of lithofacies. Lens cap is 5 cm in diameter. (A) Planar cross-stratification in lower-medium sandstone (Sp); (B) Small sub-rounded to sub-angular matrix supported clasts (Gh); (C) Clean blue well sorted siltstone, not well bedded (Fm) (D) Structureless sandstone (Sm); (E) Small-scale cross-lamination flat foresets in fine grained sandstone (Sr); (F) Small-scale cross-lamination inclined foresets in fine grained sandstone (Sr); (G) Convolute lamination and inclined foresets in upper fine sandstones

(Sd); (H) Soft sediment deformation, water escape structures in chaotic very sandstones and siltstones (Fd); (I) Poorly sorted cleaner siltstone, more organic-rich example not shown (Fp); (J) Laminated organic rich siltstone (Fl); (K) well to moderately sorted, rooted siltstone (Fr); (L) Coals with fragments of anthracite coals (C).

Figure 5. Correlation panel of 11 logged sections at Tuscher Canyon site. Surfaces and beds marked with a bold line have been walked out in field whereas dashed lines have been correlated by observation from distant vantage points in the field. This correlation panel shows the raw data collected. This outcrop “window” was used to determine a minimum extrapolated value for the dimensions of these splay elements (see methodology).

Figure 6. (A) Schematic graphic logs depicting the sedimentary signature of crevasse channel, proximal, medial and distal parts of crevasse-splay elements, as well as adjoining floodplain elements. The figure depicts lateral variations in facies and thickness across an average dip-section of a crevasse-splay. Thickness and length scales based on analysis of 35 and 20 crevasse-splay elements respectively from the studied sites in the Castlegate and Neslen formations. (B) Average, minimum and maximum thickness of each element and facies-belt type; data based on 62 measured sections from 35 crevasse-splay bodies. (C) Pie charts depicting the proportions of facies types present in each element or facies-belt type; data are based on averaged thickness data and facies type occurrences from

each of the 62 measured sections. See Table 1 for facies codes cited in key.

Figure 7. Diagram depicting typical vertical facies arrangements in each element and facies-belt type, based on average thickness occurrences. Data from 62 sections logged as part of this study. (A). Crevasse-channel. (B) Proximal splay. (C) Medial splay. (D) Distal splay. E. Floodplain. See Table 1 for facies codes cited in key.

Figure 8. Relative abundance of different element and facies-belt types at each studied site. Castlegate Sandstone sites are the Floy and Horse canyons (Fig. 3B); Neslen Formation sites are Crescent Canyon sites and Tuscher Canyon sites (Fig. 3B).

Figure 9. (A) Palaeoflow represented by the black (strike), grey (oblique) and white (dip) segments of the circle has been used to reconstruct the original crevasse-splay orientation. (B) Schematic rendering of shape of bodies used for volume modelling purposes. (C) Schematic rendering of different sections through a crevasse-splay element in plan view. (D) Graph plotting true, apparent and incomplete widths and lengths versus maximum thickness of each associated crevasse-splay element using from this study. This graph also plots maximum recorded lateral extents (unspecified orientation) from other works. See Table 2 for details of other datasets (E). Graph plotting average and range of lateral extents of each facies belt for dip and strike sections.

Figure 10. Block model depicting the typical occurrence of crevasse-splay elements within the overall succession. The model has been constructed based primarily on data from the Tuscher Canyon sections (see Fig. 5). Crevasse-splay facies-belt extents are shown, as is the inter-digitation of the distal parts of crevasse-splay elements with floodplain elements. See Table 1 for facies codes cited in key.

Table 1. Lithofacies recorded in Castlegate Sandstone and Neslen Formation study areas. See Figure 4 for photographic examples of each lithofacies.

Table 2. Comparative studies from published studies on crevasse splay dimensions in ancient successions and modern settings.

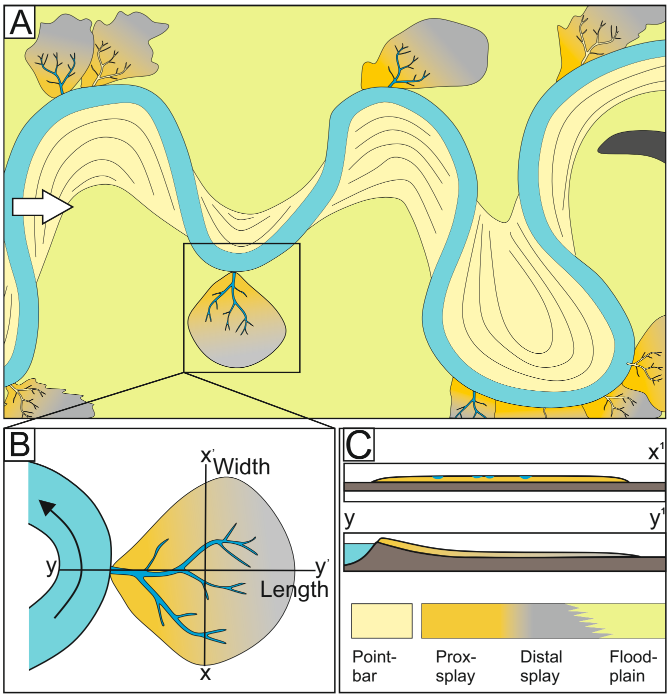
A
B
x'
Width
y
y'
Length
x
C
x'
y
y'
Point-bar
Prox-splay
Distal splay
Flood-plain

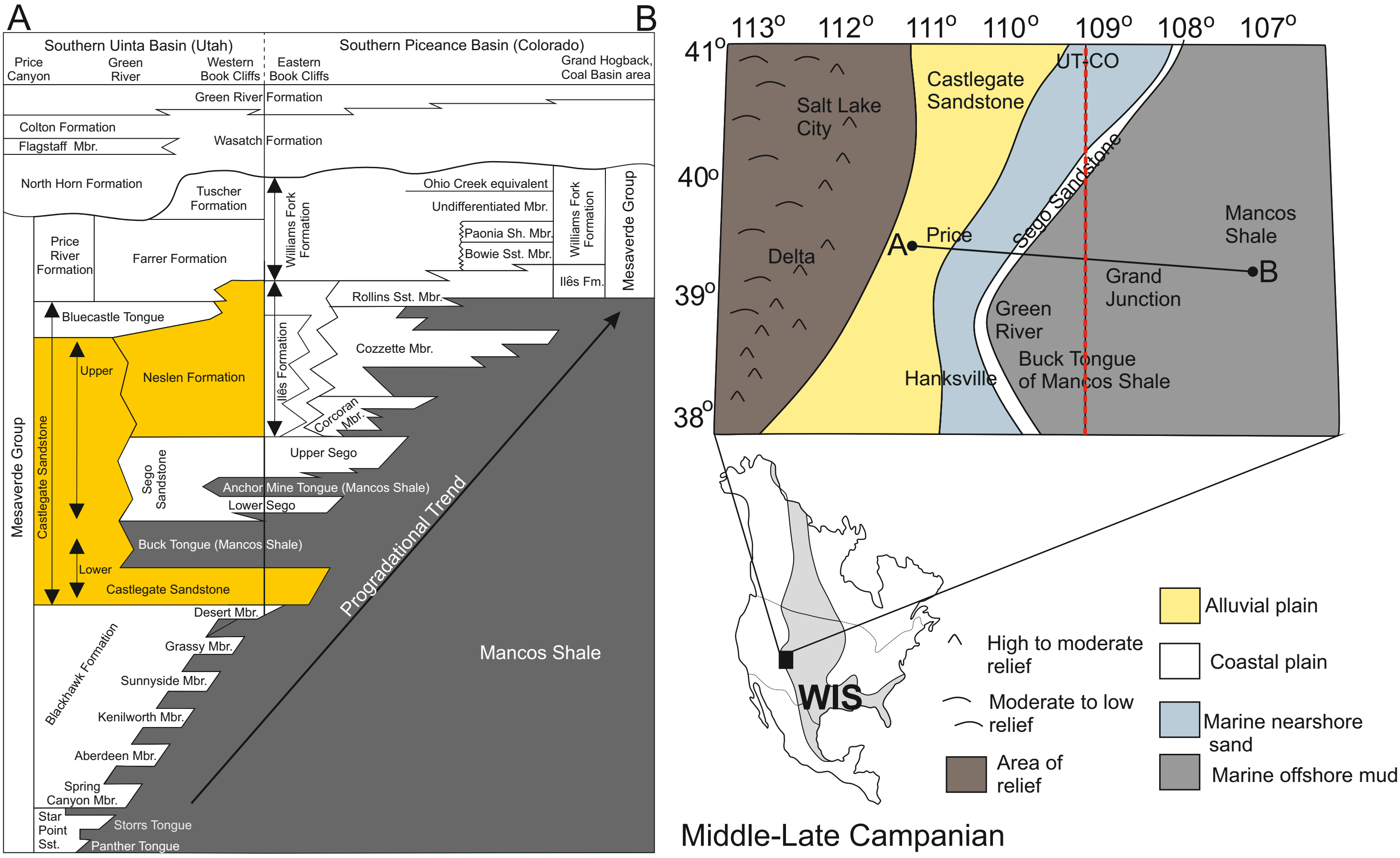

A
B
Southern Uinta Basin (Utah)
Southern Piceance Basin (Colorado)
Price Canyon
Green River
Western Book Cliffs
Eastern Book Cliffs
Grand Hogback, Coal Basin area
Green River Formation
Colton Formation
Flagstaff Mbr.
Wasatch Formation
North Horn Formation
Tuscher Formation
Ohio Creek equivalent
Undifferentiated Mbr.
Paonia Sh. Mbr.
Bowie Sst. Mbr.
Williams Fork Formation
Mesaverde Group
Price River Formation
Farrer Formation
Ilês Fm.
Rollins Sst. Mbr.
Bluecastle Tongue
Cozzette Mbr.
Upper
Neslen Formation
Ilês Formation
Corcoran Mbr.
Castlegate Sandstone
Sego Sandstone
Upper Sego
Anchor Mine Tongue (Mancos Shale)
Lower Sego
Buck Tongue (Mancos Shale)
Lower
Castlegate Sandstone
Progradational Trend
Desert Mbr.
Grassy Mbr.
Blackhawk Formation
Sunnyside Mbr.
Kenilworth Mbr.
Aberdeen Mbr.
Spring Canyon Mbr.
Star Point Sst.
Storrs Tongue
Panther Tongue
Mancos Shale
113°
112°
111°
110°
109°
108°
107°
41°
40°
39°
38°
Salt Lake City
Castlegate Sandstone
UT-CO
Sego Sandstone
Mancos Shale
Delta
Price
Grand Junction
Green River
Buck Tongue of Mancos Shale
Hanksville
WIS
High to moderate relief
Moderate to low relief
Area of relief
Alluvial plain
Coastal plain
Marine nearshore sand
Marine offshore mud
Middle-Late Campanian

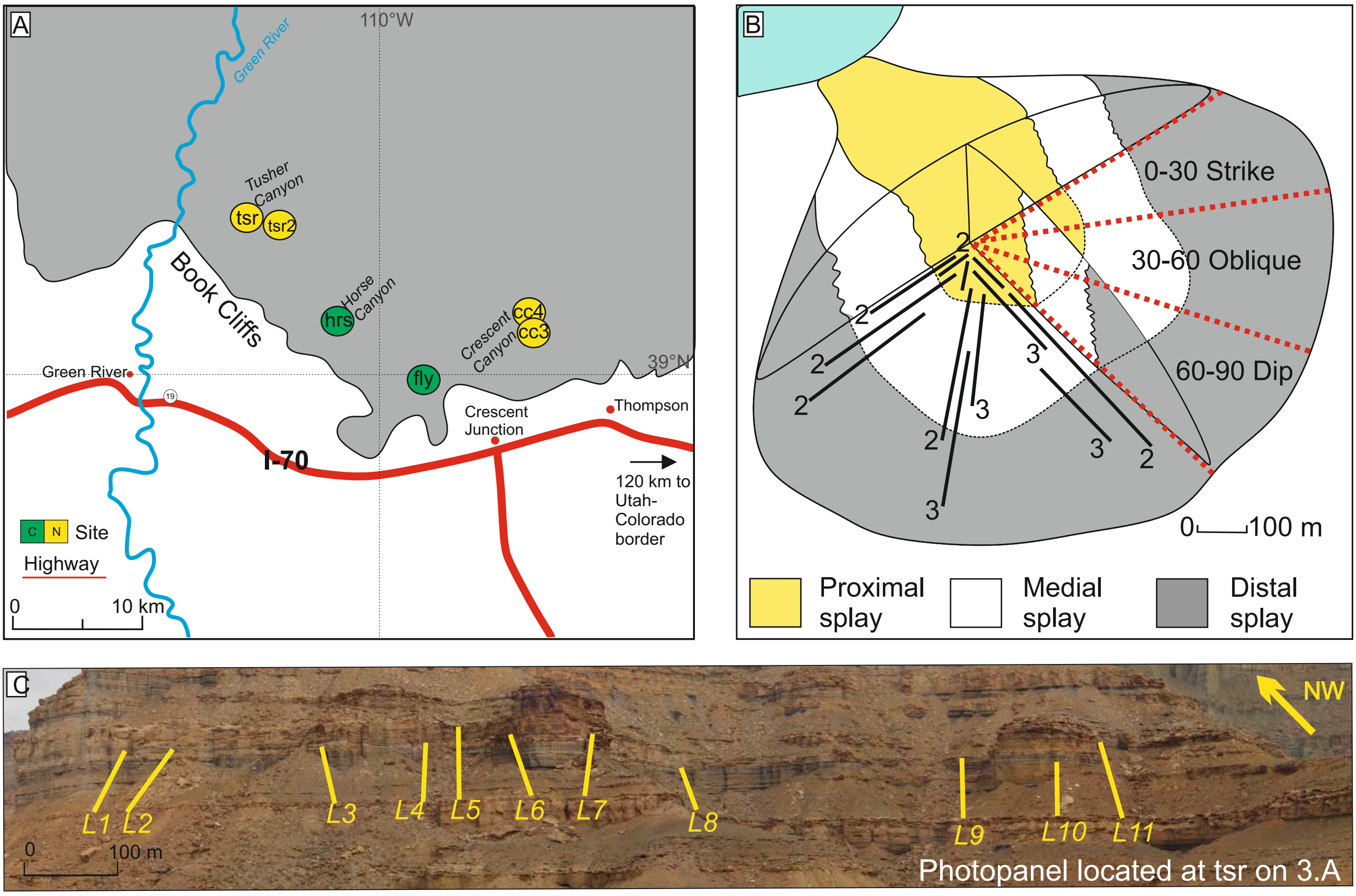

A
110°W
Green River
Tusher Canyon
tsr
tsr2
Book Cliffs
Horse Canyon
hrs
Crescent Canyon
cc4
cc3
fly
39°N
Green River
19
Crescent Junction
Thompson
I-70
120 km to Utah-Colorado border
C
N
Site
Highway
0
10 km
B
0-30 Strike
30-60 Oblique
60-90 Dip
0
100 m
Proximal splay
Medial splay
Distal splay
C
NW
L1
L2
L3
L4
L5
L6
L7
L8
L9
L10
L11
0
100 m
Photopanel located at tsr on 3.A

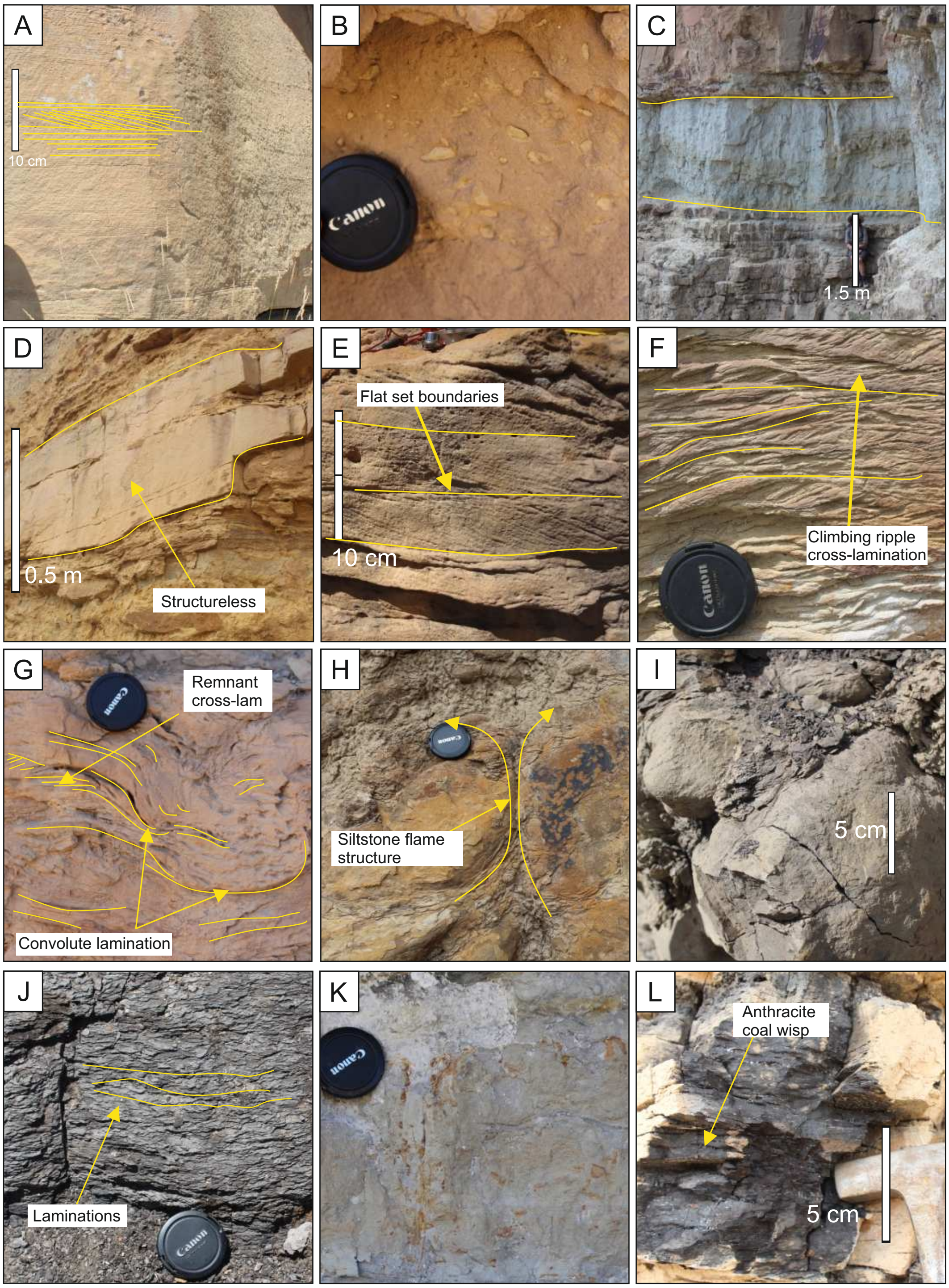
A
10 cm
B
Canon
C
1.5 m
D
0.5 m
Structureless
E
Flat set boundaries
10 cm
F
Climbing ripple cross-lamination
Canon
G
Remnant cross-lam
Convolute lamination
H
Siltstone flame structure
I
5 cm
J
Laminations
K
L
Anthracite coal wisp
5 cm

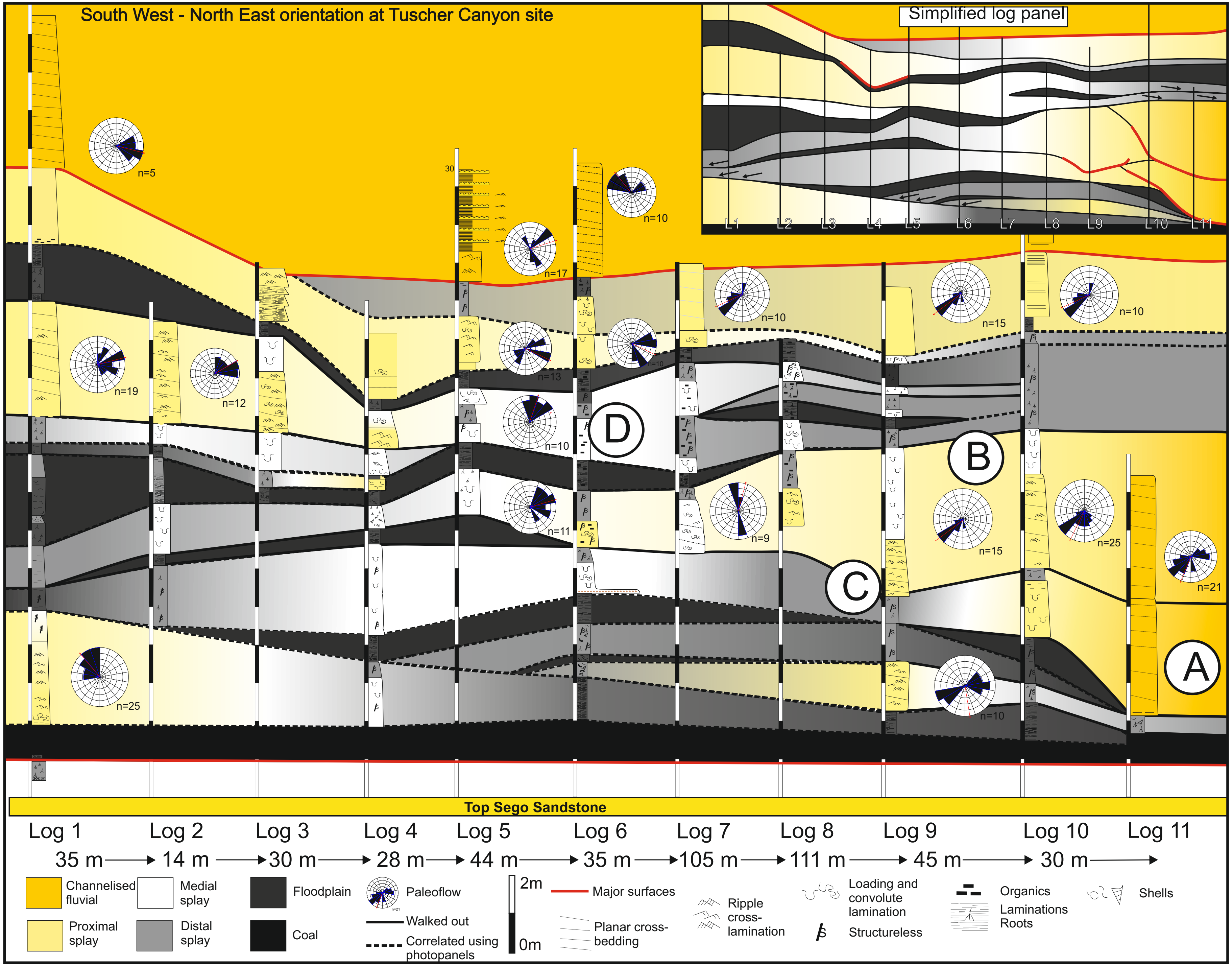

South West - North East orientation at Tuscher Canyon site
Simplified log panel
L1
L2
L3
L4
L5
L6
L7
L8
L9
L10
L11
n=5
n=19
n=12
n=25
n=17
n=13
n=10
n=11
n=10
n=10
n=9
n=15
n=15
n=10
n=10
n=25
n=21
30
A
B
C
D
Top Sego Sandstone
Log 1
Log 2
Log 3
Log 4
Log 5
Log 6
Log 7
Log 8
Log 9
Log 10
Log 11
35 m
14 m
30 m
28 m
44 m
35 m
105 m
111 m
45 m
30 m
Channelised fluvial
Medial splay
Floodplain
Paleoflow
2m
0m
Major surfaces
Ripple cross-lamination
Loading and convolute lamination
Organics
Shells
Proximal splay
Distal splay
Coal
Walked out
Correlated using photopanels
Planar cross-bedding
Structureless
Laminations
Roots

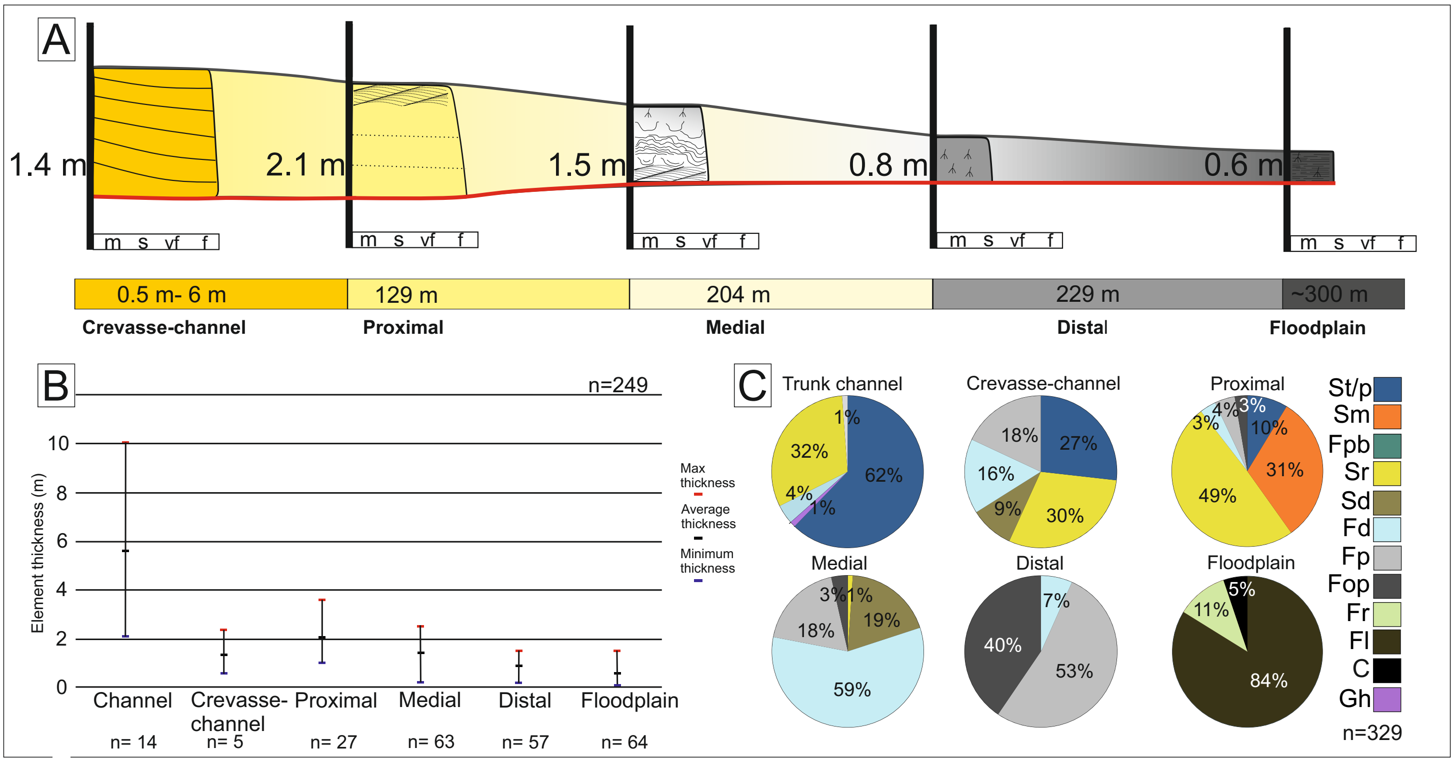
A
1.4 m
2.1 m
1.5 m
0.8 m
0.6 m
m s vf f
0.5 m- 6 m
129 m
204 m
229 m
~300 m
Crevasse-channel
Proximal
Medial
Distal
Floodplain
B
n=249
Element thickness (m)
Max thickness
Average thickness
Minimum thickness
Channel
Crevasse-channel
Proximal
Medial
Distal
Floodplain
n= 14
n= 5
n= 27
n= 63
n= 57
n= 64
C
Trunk channel
Crevasse-channel
Proximal
Medial
Distal
Floodplain
St/p
Sm
Fpb
Sr
Sd
Fd
Fp
Fop
Fr
Fl
C
Gh
n=329

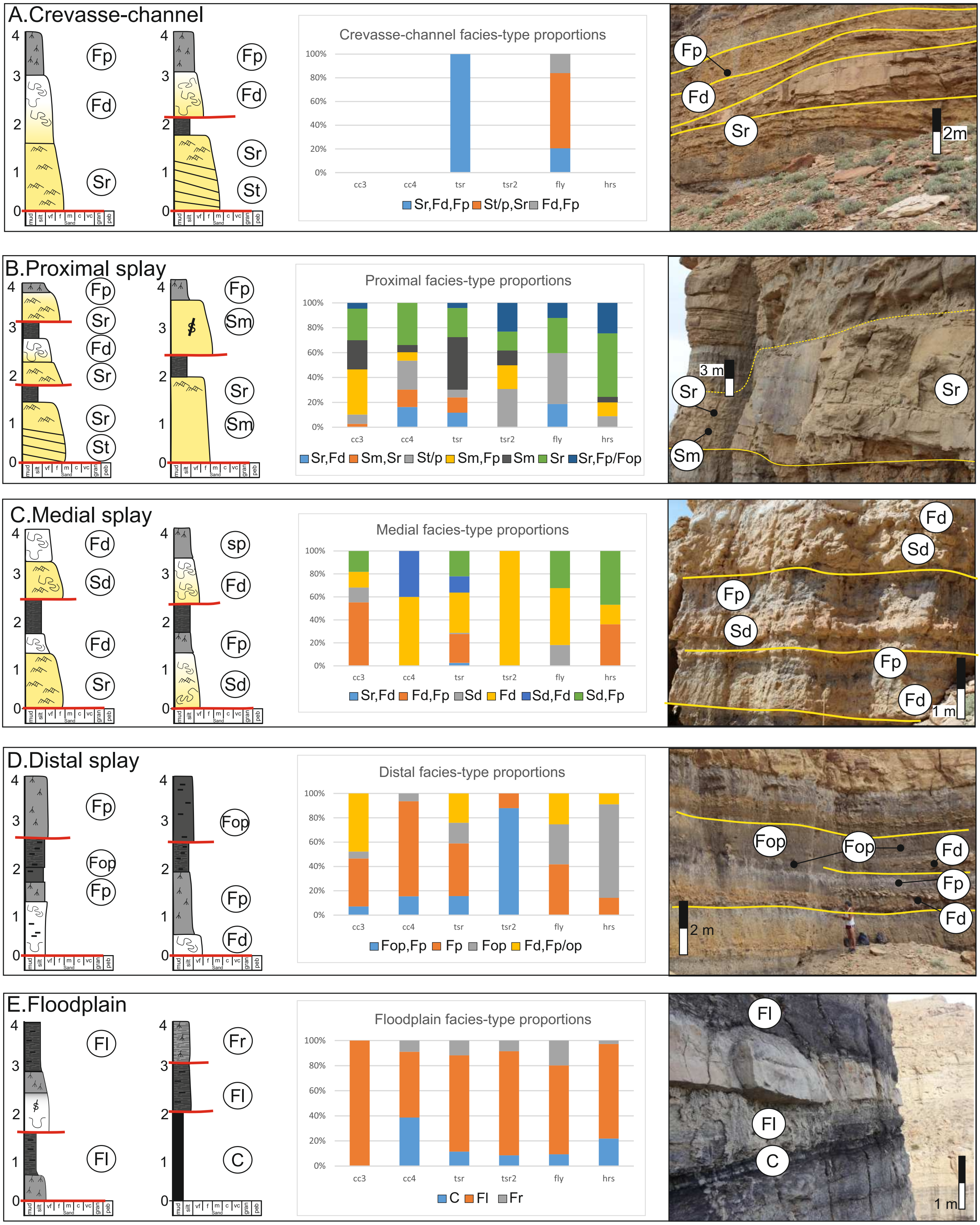

A.Crevasse-channel
Crevasse-channel facies-type proportions
Sr,Fd,Fp St/p,Sr Fd,Fp
Fp
Fd
Sr
St
2m
B.Proximal splay
Proximal facies-type proportions
Sr,Fd Sm,Sr St/p Sm,Fp Sm Sr Sr,Fp/Fop
Sm
3 m
C.Medial splay
Medial facies-type proportions
Sr,Fd Fd,Fp Sd Fd Sd,Fd Sd,Fp
sp
1 m
D.Distal splay
Distal facies-type proportions
Fop,Fp Fp Fop Fd,Fp/op
Fop
2 m
E.Floodplain
Floodplain facies-type proportions
C Fl Fr
Fl
Fr
C
1 m
cc3 cc4 tsr tsr2 fly hrs
0% 20% 40% 60% 80% 100%
mud silt vf f m c vc gran peb
Sand

n=329

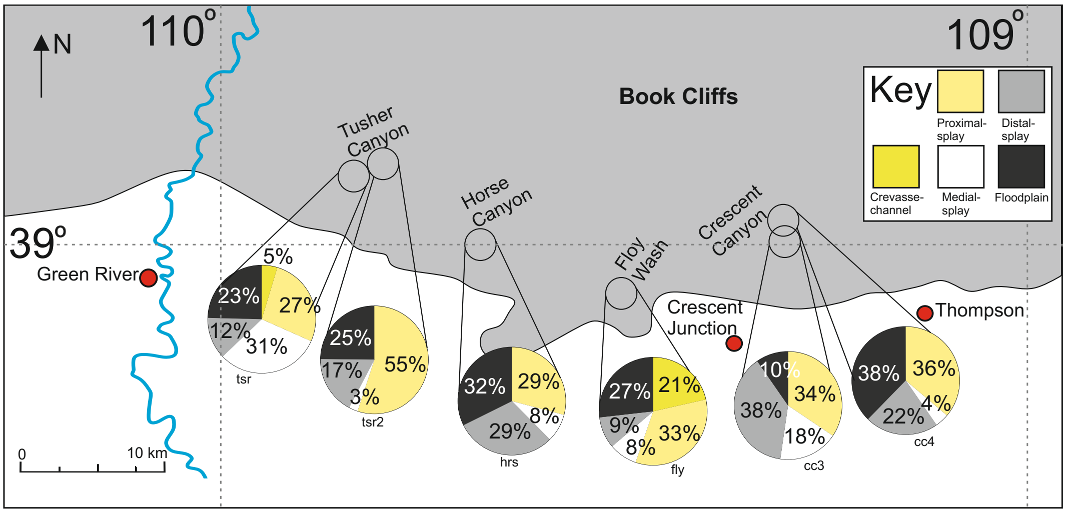

N
110°
109°
39°
Book Cliffs
Key
Proximal-splay
Distal-splay
Crevasse-channel
Medial-splay
Floodplain
Tusher Canyon
Horse Canyon
Floy Wash
Crescent Canyon
Green River
Crescent Junction
Thompson
0
10 km
5%
23%
27%
12%
31%
tsr
25%
55%
17%
3%
tsr2
32%
29%
8%
29%
hrs
27%
21%
9%
8%
33%
fly
10%
34%
38%
18%
cc3
38%
36%
4%
22%
cc4

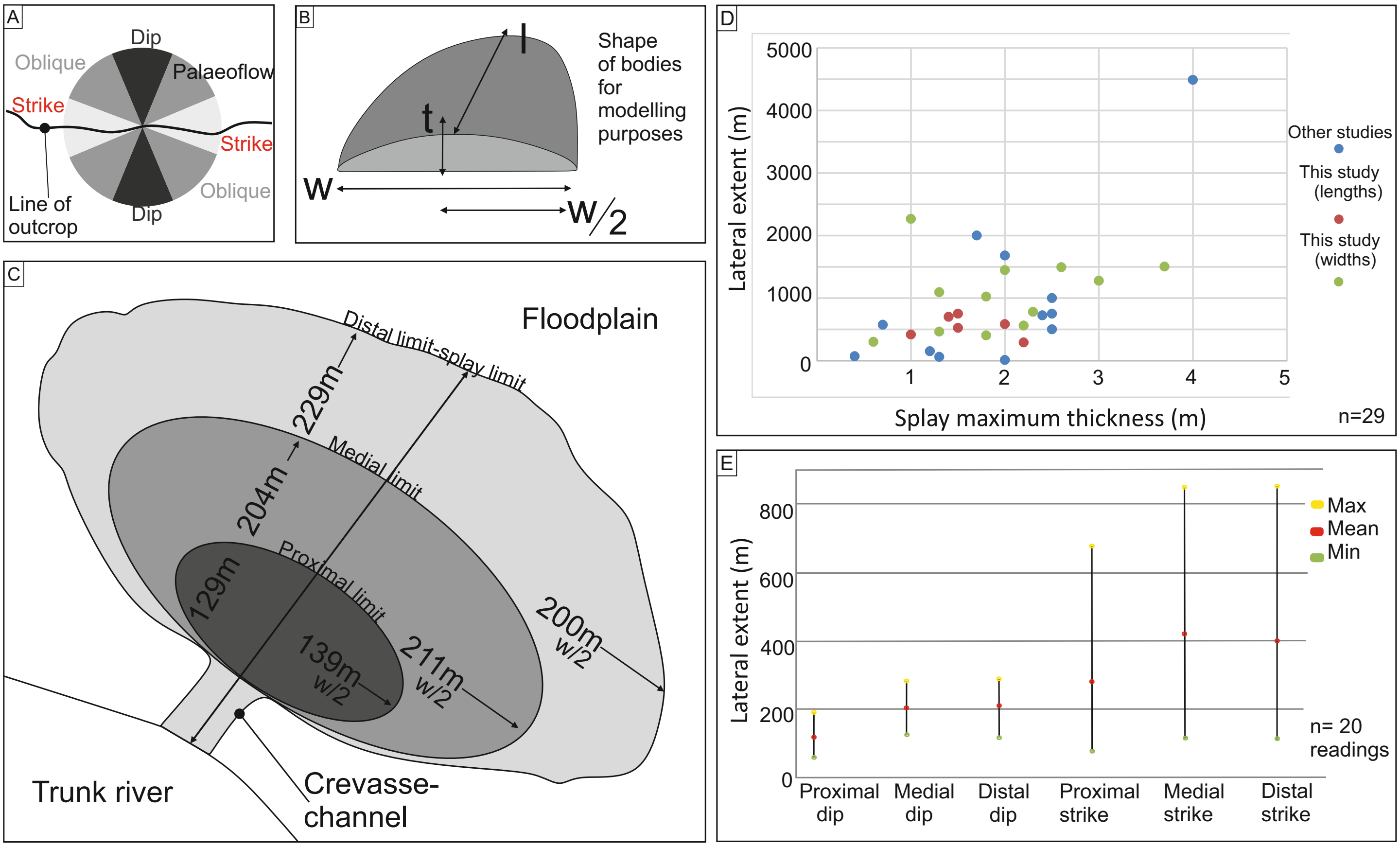

A
Dip
Oblique
Palaeoflow
Strike
Strike
Oblique
Line of outcrop
Dip
B
Shape of bodies for modelling purposes
l
t
W
W/2
C
Floodplain
Distal limit-splay limit
229m
Medial limit
204m
Proximal limit
129m
139m w/2
211m w/2
200m w/2
Trunk river
Crevasse-channel
D
Lateral extent (m)
Splay maximum thickness (m)
Other studies
This study (lengths)
This study (widths)
n=29
E
Lateral extent (m)
Max
Mean
Min
n= 20 readings
Proximal dip
Medial dip
Distal dip
Proximal strike
Medial strike
Distal strike

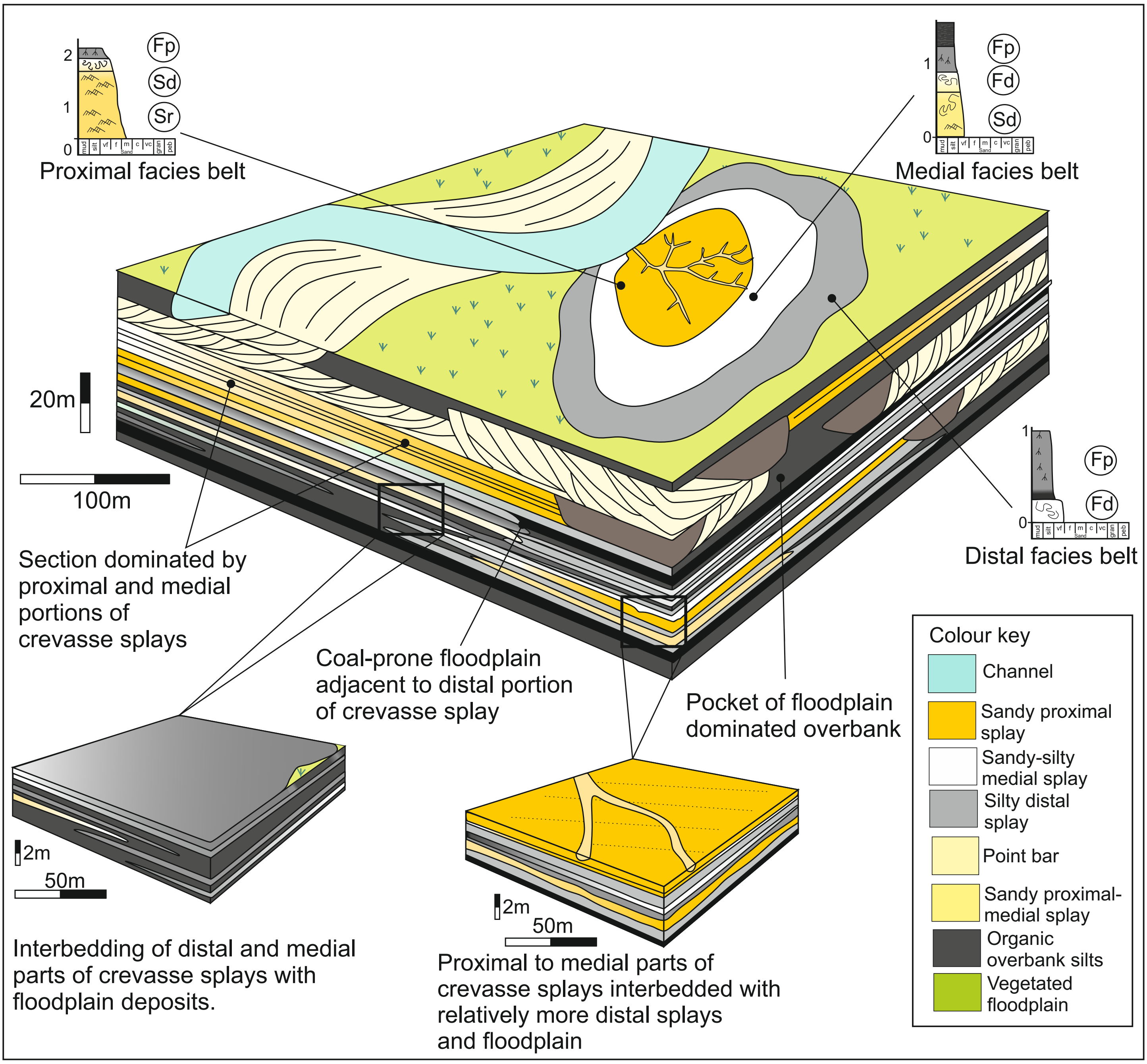
Fp
Sd
Sr
Proximal facies belt
Fp
Fd
Sd
Medial facies belt
Fp
Fd
Distal facies belt
20m
100m
Section dominated by proximal and medial portions of crevasse splays
Coal-prone floodplain adjacent to distal portion of crevasse splay
Pocket of floodplain dominated overbank
2m
50m
Interbedding of distal and medial parts of crevasse splays with floodplain deposits.
2m
50m
Proximal to medial parts of crevasse splays interbedded with relatively more distal splays and floodplain
Colour key
Channel
Sandy proximal splay
Sandy-silty medial splay
Silty distal splay
Point bar
Sandy proximal-medial splay
Organic overbank silts
Vegetated floodplain

Code	Facies	Description	Interpretation
Ft/Fp	Trough and planar cross-bedded sandstone	Grey-yellow, medium- to very-fine grained sandstone, moderately well sorted with subangular to subrounded grains. Comprises 12.8% of logged thickness of type succession. Sets are 0.5 to 0.8 m thick. Mud rip-up clasts and plant fragments are common. Trough and planar cross-stratification throughout.	Deposition rapidly from a relatively high-energy flow; downstream migration of sandy bar forms (Allen, 1963; Rubin, 1987; Rubin and Carter, 2006).
Gh	Pebbly sandstone with intraformational clasts	Brown to grey-yellow. Very-fine sandstone matrix supporting rounded small to medium pebbles (up to 20 mm in diameter). Comprises 0.6% of logged thickness of type succession. Sets of this facies are <1 m thick. Pebbles are poorly sorted as is the sandstone matrix; no grading is present; sets are Structureless. Typically overlies erosional bounding surfaces.	Deposition from a very high-energy environment, within which flows were capable of entraining and reworking locally derived sediment locally as clasts. Occurrence of this facies directly above major erosional bounding surfaces indicates that it represents a lag deposit at the base of the channel (Farrell, 19878; Collinson et al., 2006).
Sm	Structureless sandstone	Dark grey-yellow, fine to very-fine sandstone, moderately to poorly sorted. Thickness ranges 0.5 to 3 m; Comprises 12.3% of logged thickness of type succession. Internally sets are structureless	Records rapid deposition of sand predominantly from suspension in a decelerating flow where the rate of deposition was too rapid to allow primary structures to form (Jones and Rust, 1983)
Sr	Small-scale ripple cross-laminated sandstone	Grey-yellow, fine to very fine sandstone, moderately to poorly	Downstream migration of ripple

		sorted. Sets vary from 0.5 to 2 m. Bedset bases are sharp are generally non-erosive, however gutter casts are present in some places. Comprises 9.1% of logged thickness of type succession. Small-scale ripple- cross lamination is common(4 – 10 cm set thickness), contains small (<50 mm long) plant fragments, bark pieces and coal fragments.	bedforms under an aggradational regime
Sd	Soft-sediment deformed sandstone with remnant ripple forms	Grey-yellow, very fine sandstone that is moderately sorted. Sets vary in thickness from 0.5 to 3 m. Comprises 11.4% of logged thickness of type succession. Convolute lamination within sets and load and flame structures at base bed boundaries, occasional disturbed ripple forms.	Records deposition from flow an unstable water-saturated substrate. Convolute lamination indicates plastic deformation of water-saturated, non-consolidated sediment during or soon after deposition (Allen, 1977; Collinson et al 2006, p. 197-198).
Fd	Soft-sediment deformed mixed sandstone and siltstone	Dark grey-yellow, upper-very fine sandstone and coarse siltstone that is poorly sorted. Set thicknesses vary from 0.3 to 3 m. Comprises 18% of logged thickness of type succession. Within ~1 m of the base of sets, any primary sedimentary structures are overprinted by soft-sediment deformation structures e.g upward-	Records deposition from a flow containing poorly sorted small grains onto an unstable water-saturated substrate. The more silt-prone, waterlogged, parts of sets became overpressured in response to loading. Which led to expulsion of fluids when pore pressure was high enough to breach overlying

		oriented water-escape structures	sediment (Allen 1977; Owen, 1978).
Fp/Fop	Structureless, poorly-sorted rooted siltstone	Light-blue(Fp) or dark grey (Fop), very fine sandstone to fine siltstone that is poorly sorted. Set thicknesses vary from 0.3 to 1.1 m (mean is 0.5 m). Comprises 22.2% of logged thickness of type succession. Sets of this facies are mostly structureless though some show weak fining-up trend.Both subfacies have in-situ roots. Fop has greater dispersed organic content and more roots than Fp.	Poorly sorted and structureless silt-prone facies was deposited rapidly from suspension. The occurrence of in-situ roots supports the interpretation of a non-channelszed setting (Marconato et al., 2013). Greater organic content of Fop reflects both organic content of flow in trunk channel and entrainment of organic matter on floodplain (Kelle and Swanson, 1979; Hein et al., 2003).
Fl	Laminated, organic-rich siltstone	Medium to dark grey, fine siltstones well to moderately sorted; set thicknesses vary from 0.1 -1.6 m, 53 cm average grain remains consistent throughout a set. Comprises 11.1% of logged thickness of type succession. Planar lamination common. Small plant roots (<10mm) and thin anthracite coal wisps (2- 50 mm).	Steady continues deposition from low-energy flow onto planar, near horizontal substrate (Collinson et al., 2006, p. 70). Coal fragments could have been incorporated as detritus from other areas of overbank (Retallack 1988; Kraus, 1999).
Fr	Laminated, rooted siltstone	Blue grey to light grey, upper to lower silt moderately well sorted, average set thicknesses 0.7 m but bed size varies from 0.3 to 1.4 m. Comprises 0.6% of logged thickness of type succession. Weakly laminated. Plant-root structures are common, but are	Gradual deposition under low-energy regime onto well-drained substrate. Records development of a protosol: organic matter present as roots and weak horisonation (cf. Mack et al., 1993). Indicates rate of sediment aggradation that is low enough to allow

		concentrated in the uppermost parts of bedsets. Roots narrow down, composed of siderite, 1 – 5 mm thick, 5 -10 cm long.	pedogenesis and absence of significant erosion.
Fm	Well sorted, blue, clean siltstone	Light blue, medium to coarse siltstone, well to moderately-well sorted; rare occurrence of roots or plant material. Set bases show an erosional relief of 1-2 m. Average set thickness 2 m (Rarely up to 3 m). Comprises 0.3% of logged thickness of type succession. Siltstone can be weakly laminated or structureless	Erosional relief on set bases record erosive flow; siltstone represents deposition from low energy flow after erosional event (cf. Toonen et al., 2012).
Fc	Coal	Dark-grey to black clay sized particles, well sorted, sets vary from 0.4 to 0.9 m. Comprises 1.6% of logged thickness of type succession .Plant remains present and anthracite coal fragments common. But mostly a poorer quality lignite or sub-bituminous coal.	Records slow deposition in an organic-rich setting with limited clastic input(McCabe, 1987; Kirschbaum and Hettinger, 2004; Cole, 2008). Accumulated in a waterlogged swamp (Shiers et al., 2014).

Maximum thickness (m)	Maximum lateral extent (m)	Average channel Thickness (m)	Average channel Widths (m)	Case study
0.4	70	1	5	O'Brien and Wells, 1986
0.7	575	–	–	Farrell, 2003
1.2	150	–	250	Bristow et al., 1999
1.3	60	10	–	Anderson, 2005
1.7	2000	1.7	150	Fisher et al., 2008
2	1680	6.5	135	Arnaud-Fassetta, 2013
2	10	7	–	Rhee et al., 1993
2.4	725	17	80	This study length values
2.5	500	–	650	Mjos et al., 1993
2.5	1000	–	250	Bristow et al.,1999
2.5	750	–	–	Toonen et al., 2015
4	4490	6.5	135	Arnaud-Fassetta, 2013